



**HAL**  
open science

# Abiotic transformation of polycyclic aromatic hydrocarbons via interaction with soil components: A systematic review

Jinbo Liu, Chi Zhang, Hanzhong Jia, Eric Lichtfouse, Virender Sharma

## ► To cite this version:

Jinbo Liu, Chi Zhang, Hanzhong Jia, Eric Lichtfouse, Virender Sharma. Abiotic transformation of polycyclic aromatic hydrocarbons via interaction with soil components: A systematic review. *Critical Reviews in Environmental Science and Technology*, 2023, 53, pp.676-699. 10.1080/10643389.2022.2083897. hal-03690995

**HAL Id: hal-03690995**

**<https://hal.science/hal-03690995v1>**

Submitted on 8 Jun 2022

**HAL** is a multi-disciplinary open access archive for the deposit and dissemination of scientific research documents, whether they are published or not. The documents may come from teaching and research institutions in France or abroad, or from public or private research centers.

L'archive ouverte pluridisciplinaire **HAL**, est destinée au dépôt et à la diffusion de documents scientifiques de niveau recherche, publiés ou non, émanant des établissements d'enseignement et de recherche français ou étrangers, des laboratoires publics ou privés.

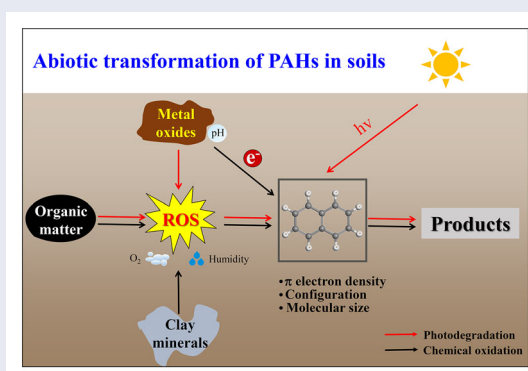
## Abiotic transformation of polycyclic aromatic hydrocarbons via interaction with soil components: A systematic review

Jinbo Liu<sup>a</sup>, Chi Zhang<sup>a</sup>, Hanzhong Jia<sup>a</sup>, Eric Lichtfouse<sup>b</sup>, and Virender K. Sharma<sup>c</sup>

<sup>a</sup>Key Laboratory of Plant Nutrition and the Agri-environment in Northwest China, Ministry of Agriculture, College of Natural Resources and Environment, Northwest A & F University, Yangling, China; <sup>b</sup>Aix-Marseille Univ, CNRS, IRD, INRA, CEREGE, Aix-en-Provence, France; <sup>c</sup>Program for the Environment and Sustainability, Department of Occupational and Environmental Health, School of Public Health, Texas A&M University, College Station, TX, USA

### ABSTRACT

Natural attenuation is a major ecosystem function allowing to abate soil organic contaminants such as polycyclic aromatic hydrocarbons (PAHs). Biodegradation of PAHs is classically considered as the major driver of natural attenuation, yet the role of abiotic transformation, including photodegradation, chemical oxidation, formation of non-extractable residues, and polymerization, has been overlooked due to the lack of investigations until recently. This paper reviews PAHs dissipation in soils by abiotic processes such as photodegradation and oxidation catalyzed by inorganic





minerals and organic matters. The role of soil components on degradation rates, pathways, and mechanisms are discussed. The products of PAHs abiotic transformation and their potential risks are also described. Abiotic transformations are mainly controlled by interactions between PAHs and clay minerals, metal oxides/hydroxides, and soil organic matter. PAH photodegradation proceeds by both direct and indirect photolysis processes, which are enhanced in the presence of natural photosensitizers, for example, organic matter, and photocatalysts, for example, metal oxides/hydroxides. PAHs can also be chemically/catalytically oxidized by metal oxides/hydroxides, for example, MnO<sub>2</sub>, FeO<sub>2</sub>, and clay minerals without light irradiation. Overall, PAHs transformation depends on their electron-donating properties, mineral electron-accepting properties, pH, temperature, moisture, and oxygen content. Following the elucidation of the transformative mechanism, knowledge to understand the impact of abiotic transformation on biodegradation are delineated. Future investigations are needed to advance the correlation of laboratory generated rates to the field applications, and the potential applications of natural attenuation based on abiotic processes are proposed.

**Abbreviations:** PAHs: polycyclic aromatic hydrocarbons; SOM: soil organic matter; DOM: dissolved organic matter; HA: humic acid; FA: fulvic acid; HM: humin; NERs: non-extractable residues; <sup>1</sup>O<sub>2</sub>: singlet oxygen; O<sub>2</sub><sup>•-</sup>: superoxide anion radical; •OH: hydroxyl radical; EPFRs: environmentally persistent free radicals; ROS: reactive oxygen species; IP: ionization potential; E<sub>HOMO</sub>: energy highest occupied molecular orbital; E<sub>LUMO</sub>: energy lowest unoccupied molecular orbital

**KEYWORDS** Abiotic transformation; polycyclic aromatic hydrocarbons; photodegradation; chemical oxidation; soil components

**HANDLING EDITORS** Dan Tsang and Yong Sik Ok

**CONTACT** Hanzhong Jia  [jjahz@nwfau.edu.cn](mailto:jjahz@nwfau.edu.cn)  Key Laboratory of Plant Nutrition and the Agri-environment in Northwest China, Ministry of Agriculture, College of Natural Resources and Environment, Northwest A & F University, Yangling 713010, China.

Supplemental data for this article is available online at <https://doi.org/10.1080/10643389.2022.2083897>.

## 1. Introduction

Polycyclic aromatic hydrocarbons (PAHs) are organic compounds that contain of two or more benzene rings with various structural configurations. The chemical structures of the 16 PAHs considered as priority pollutants are given in [Figure S1](#) (Supporting information). PAHs are produced by natural sources, for example, forest fires, volcanic eruptions and oil seeps, and by anthropogenic sources, for example, burning of fossil fuel, municipal solid waste incineration and petroleum spills (Samanta et al., 2002; Haritash & Kaushik, 2009). PAHs occur ubiquitously in soils, sediments, plants, food, waters, and atmosphere at various concentrations ranging from  $\sim 10 \text{ ng g}^{-1}$  to  $1000 \mu\text{g kg}^{-1}$  (Bryselbout et al., 2000; Eriksson et al., 2000; Grova et al., 2000; Samanta et al., 2002). Nearly 90% of PAHs in natural phases finally end up into soils by wet and dry deposition, wastewater discharge, and disposal of solid waste (Wild & Jones, 1995; Eriksson et al., 2000). The concentration of PAHs in soils vary from sub  $\mu\text{g kg}^{-1}$  to tens of thousands of  $\text{mg kg}^{-1}$ , depending on the source of contamination (Eriksson et al., 2000; Kanaly & Harayama, 2000). Once entering the soil, PAHs may be preserved for a long time by protection into soil particles (Lichtfouse et al., 1997). In addition, many PAHs are toxic, mutagenic, and carcinogenic (Samanta et al., 2002). Therefore, the environmental behavior and fate of PAHs in soil are raising increasing attention because of their environmental persistence and potential harm to human health.

Natural attenuation refers to natural processes—as opposed to anthropic processes—that reduce the amount and toxicity of contaminants under natural conditions. Natural attenuation is a cost-effective alternative to abate organic pollutants at contaminated sites because it provides adequate conditions of PAH transformation. The fate of PAHs in the soil environment is exhibited in [Figure 1](#). Specifically, the attenuation of PAHs in soils mainly proceeds by biodegradation such as microbial degradation, and by abiotic dissipation such as volatilization, photodegradation on the soil surface, chemical oxidation on minerals, and irreversible sorption to soil organic matter and mineral pores (Harvey et al., 2002; Rababah & Matsuzawa, 2002; Rivas, 2006). Biodegradation has long been considered as the major driver of natural attenuation of PAHs (Haritash & Kaushik, 2009). Nonetheless, reports have shown that only low-molecular-weight PAHs are easily biodegraded (Wang et al., 2016; Biache et al., 2014), whereas high-molecular-weight PAHs, for example, benzo[a]pyrene, are hardly biodegraded because they are water-insoluble and toxic (Yi & Crowley, 2007; Biache et al., 2013). On the other hand, abiotic transformation of PAHs may occur more than that of current thought, notably when biological activity is relatively low (Schaefer et al., 2013; Biache et al., 2013; Duan et al., 2015). However, the

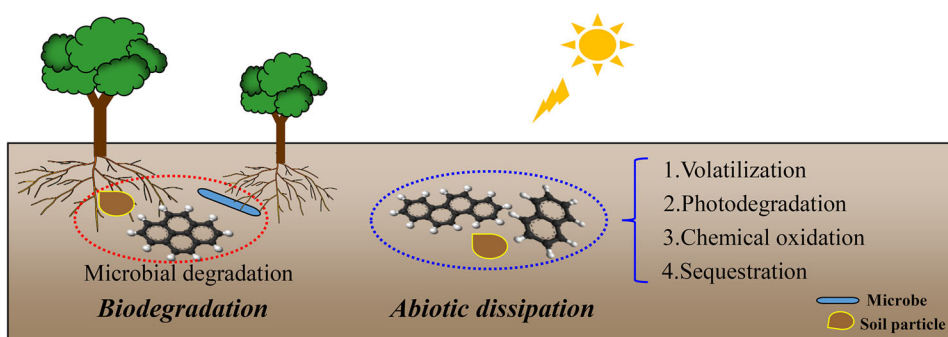


**Figure 1.** Processes controlling the fate of polycyclic aromatic hydrocarbons (PAHs) in soils. PAHs concentrations can be decreased by biodegradation and abiotic dissipation. Biodegradation mainly includes microbial degradation. Abiotic dissipation mainly includes volatilization, photodegradation, chemical oxidation and sequestration.

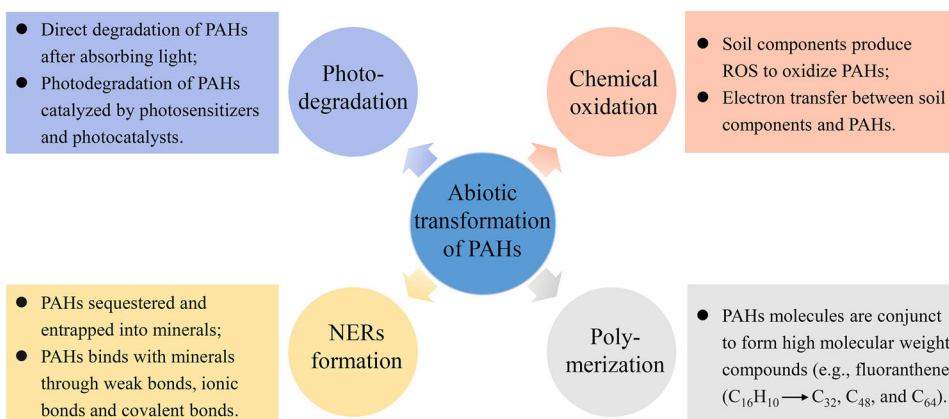


**Figure 2.** Abiotic transformation of polycyclic aromatic hydrocarbons (PAHs) in soils involves mainly volatilization, photodegradation, chemical oxidation and formation or non-extractable residues (NERs).

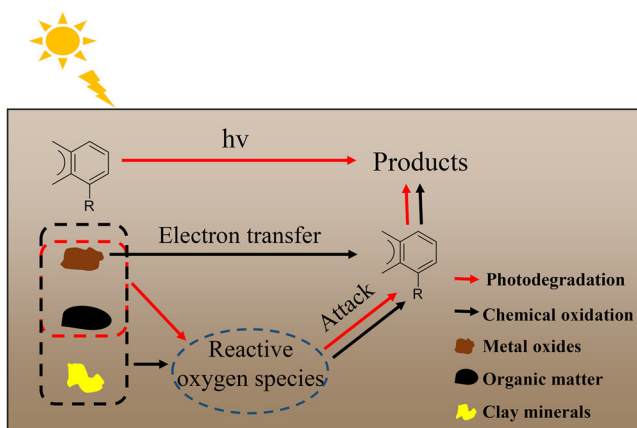


**Figure 3.** Photodegradation and chemical oxidation of polycyclic aromatic hydrocarbons (PAHs) in soils.

contribution of abiotic transformation for PAH attenuation in soils has been somewhat overlooked (Schaefer et al., 2013; Zhao et al., 2019; Ni et al., 2021).

Abiotic transformation of PAHs mainly includes photodegradation, chemical oxidation, formation of non-extractable residues (NERs), and polymerization (Figure 2, Stangroom et al., 2000; Lehner et al., 2004; Li et al., 2015; Jia et al., 2016). NERs formation means that PAHs are trapped into the organic-mineral matrix by encapsulation or chemical binding (H bonds, ionic bonds, and covalent bonds, Schaffer et al., 2018). And polymerization refers molecular condensation within PAH molecules via chemical bond, which increases the organic insoluble fraction (Biache et al., 2011). Overall, photodegradation and chemical oxidation induce the degradation/transformation of PAHs, whereas polymerization and NERs formation involve the stabilization of PAHs. Thus, photodegradation and chemical oxidation processes, as depicted in Figure 3, have been paid more attentions during the attenuation of PAHs in soil environment (Cheng et al., 2006; Jia et al., 2015; Zhao et al., 2019). These processes involve interactions between PAHs and soil components, for example, clay minerals, metal oxides/hydroxides, and soil organic matter (SOM). Soil components can act as catalysts, oxidants, and photosensitizers to promote the transformation of PAHs (Butler & Hayes, 2000; Ranc et al., 2016). Nonetheless, the precise role of soil components in PAH abiotic transformation has been poorly investigated until recently.

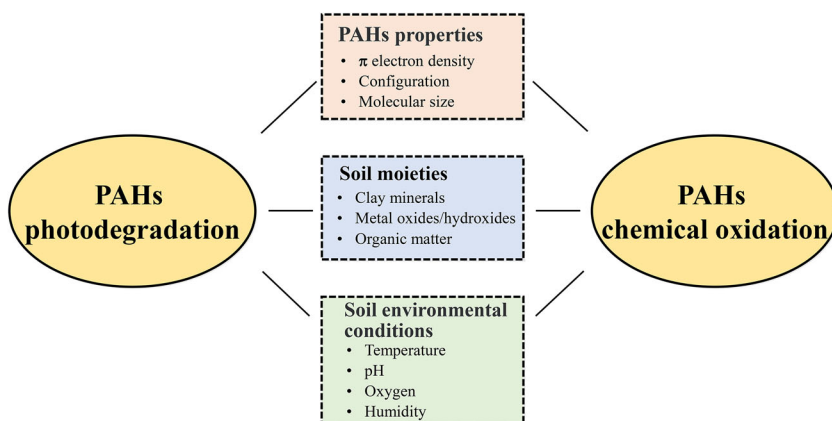


**Figure 4.** Factors influencing the photodegradation and chemical oxidation of polycyclic aromatic hydrocarbons (PAHs) in soils.

While PAH attenuation associated with biodegradation has already been thoroughly investigated and reviewed (Alegbeleye et al., 2017; Shahsavari et al., 2019; Premnath et al., 2021), the natural occurrence and applications of abiotic processes for PAHs-contaminated soil have rarely noticed. Developing natural decay techniques based on abiotic processes may, however, represent an alternative or complementary remediation technique to treat PAH-contaminated soils, notably for soils of low biological activity and high PAHs content. Moreover, better knowledge of abiotic processes controlling PAH attenuation may not only reveal the potential environmental risks of PAHs-contaminated soil, but also help to understand the attenuation of other organic pollutants. In view of the above, this article reviews the contribution of abiotic processes to the natural removal of PAHs in soils, with focus on transformation kinetics, influencing factors, intermediates, and final products. Detailed transformative pathways and underlying mechanisms are also described, with particular emphasis on the role of soil components. Finally, we identify knowledge gaps needed to upscale the application of abiotic transformation from the laboratory to field-contaminated soils.

## 2. Photodegradation of polycyclic aromatic hydrocarbons

Photodegradation is considered as a major process controlling the fate of PAHs at the upper surface soil layer (Dong et al., 2009; Dong et al., 2010; Zhang et al., 2010; Nguyen et al., 2020). Generally, the photodegradation of PAHs proceeds by direct and/or indirect photolysis (Katagi, 1990; Schwarzenbach et al., 2003; Jia et al., 2015). Due to the differences in photodegradation mechanisms, PAHs photodegradation in soils depends mainly on PAH properties, soil moieties, and soil environmental conditions (Dong et al., 2010; Zhang et al., 2010; Jia et al., 2015) (Figure 4).

### 2.1. Photodegradation mechanisms

#### 2.1.1. Direct photodegradation

Direct photolysis is a process in which PAHs absorb light directly and undergo subsequent chemical reactions (Schwarzenbach et al., 2003). After adsorption of photons, PAHs molecules shift into singlet and triplet states, which are initial reactive intermediates during the photolysis process (Eqs. (1) and (2), Lehto et al., 2003). Triple state PAHs react with triple state dioxygen to produce single state dioxygen (Eq. (3), Lehto et al., 2003). Then endoperoxide is generated during the interaction of singlet oxygen and another PAH (Fox & Olive, 1979). After that, the irradiation

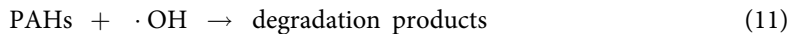
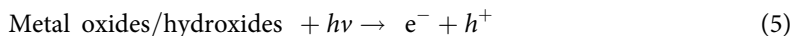
between PAHs and endoperoxide results in the formation of diones such as quinones (Eq. (4), Miller & Olejnik, 2001). Overall, irradiation may induce the break of chemical bonds and complete degradation via initial photo-absorption by PAHs (Schwarzenbach et al., 2003).



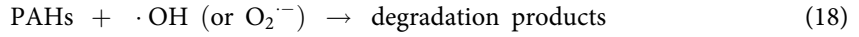
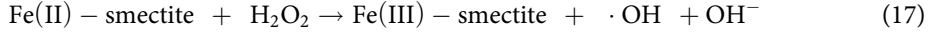
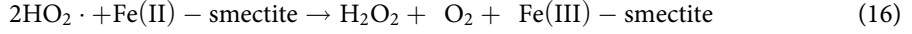
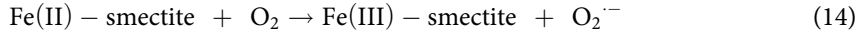
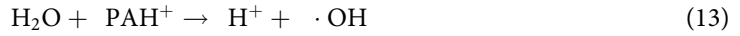
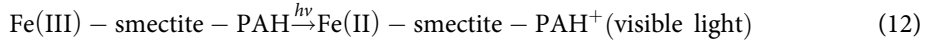
### 2.1.2. Indirect photodegradation

Indirect photolysis means that light is first absorbed by soil components to generate reactive oxygen species (ROS), which then participate in the degradation of PAHs (Schwarzenbach et al., 2003). Specifically, an indirect photochemical reaction refers to the absorption of light energy by photocatalyst or photosensitizer materials such as metal oxides/hydroxides, clay minerals, or SOM. The absorbed light energy then induces an electron transfer from soil components to adsorbed  $\text{O}_2$  and  $\text{H}_2\text{O}$ , inducing the formation of ROS such as  ${}^1\text{O}_2$ ,  $\text{O}_2^-$ , and  $\cdot\text{OH}$ , which in turn initiate the transformation of PAHs (Schwarzenbach et al., 2003).

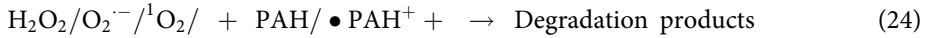
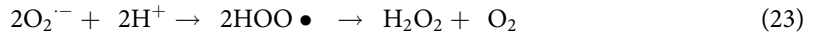
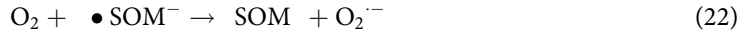
Metal oxides/hydroxides, denotes as inorganic minerals possessing photocatalytic activity and semiconducting properties, can accelerate PAHs photodegradation (Chakrabarti & Dutta, 2004). Briefly, after irradiation, metal oxides/hydroxides receive energy from the photons and are thus excited from valence band to conductive band, leading the formation of electrons and electron holes (Eq. (5), Chakrabarti & Dutta, 2004). Both electron holes and separated electrons can induce the generation of  $\text{O}_2^-$  and  $\cdot\text{OH}$  that are capable of degrading PAHs (Eqs. (6)–(11), Kong & Ferry, 2003).



The unique properties of clay minerals also induce electron migration from the surface to the core of clay matrix, enabling a stable charge separation (Huber et al., 2010). As the main reactive intermediates,  $\text{O}_2^-$  is produced by stimulating the electron transfer between clay and molecular oxygen during this process. In addition, the photodegradation of PAHs is promoted by the presence in clays of transition metal ions, for example, Fe(III) and Cu(II). Specifically, Fe(III) in smectite is reduced to Fe(II) by receiving electrons (Eq. (12)), and PAHs radical cations may be generated in the process of electron transfer (Miller & Olejnik, 2001).  $\cdot\text{OH}$  is also formed after  $\text{H}_2\text{O}$  trapping electron from  $\text{PAH}^+$  (Eq. (13)). In the presence of  $\text{O}_2$ , the produced Fe(II) is reoxidized to Fe(III) with the simultaneous formation of  $\text{O}_2^-$  and  $\text{HO}_2\cdot$  (Eqs. (14) and (15), Yap et al., 2011). The resulting  $\text{O}_2^-/\text{HO}_2\cdot$  is converted to  $\text{H}_2\text{O}_2$  by disproportionation (Eq. (16)), and then  $\cdot\text{OH}$  is generated in a system containing Fe(II) and  $\text{H}_2\text{O}_2$  by a Fenton-like reaction (Eq. (17), Goss & Eisenreich, 1996). The formed  $\cdot\text{OH}$  and  $\text{O}_2^-$  can further transform PAHs (Eq. (18), Szaćiłowski et al., 2005).



As a type of natural photosensitizer, SOM can be excited, denoted as SOM\*, after absorbing visible light (Eq. (19)) (Jia et al., 2013). On the one hand, SOM\* can react with PAHs directly, inducing the formation  $\bullet\text{PAH}^+$  (Eq. (20)). On the other hand, the excited SOM induces the formation of ROS (Eqs. (21)–(23)), which in turn enhance the photodegradation of PAHs (Eq. (24)).



## 2.2. Effects of PAH properties

The photodegradation of various PAHs in soils have been widely studied (Dong et al., 2010; Sun et al., 2011; Jia et al., 2015), and their disappearance kinetics and corresponding rate constants are compiled in Table S1. It is noted that the photodegradation rate of PAHs in soils firstly depends on the properties of PAHs molecules (Cavoski et al., 2007; Zhang et al., 2010). Specifically, the potential of photolysis highly depends on the extent of the spectral overlap between the absorption spectrum of PAHs and the emission spectrum of the beam of sunlight in the range 290-750 nm (Katagi, 1990). PAHs generally absorb photons in the visible or near ultraviolet part of the spectrum (Schwarzenbach et al., 2003). The absorption maxima are shifted to longer wavelengths with the increase in molecular weight. Therefore, high-molecular-weight PAHs are more easily transformed by direct photolysis. For instance, the half-life of naphthalene, a 2-ring compound, is 71 h whereas that of benzo[a]pyrene, a 5-ring compound, is 0.54 h under similar conditions. This is explained by the fact that high-molecular-weight PAHs match better the solar spectrum, making them prone to photolysis (Chien et al., 2011).

## 2.3. Effects of soil moieties

Soil types influence the photodegradation of PAHs. For example, the photodegradation rate of anthracene in various types soils decreases in the order of red earth > latosol ~ fluvo-aquic soil > yellow earth > chernozem ~ brown soil > calcic brown soil (Jia, Zhao, Shi, Fan, et al., 2019). The different photodegradation rate of anthracene in various soils is attributed to the varying composition of soil components. Moreover, the photodegradation of anthracene in silica powders

is less than 5%, suggesting that the soil active components, such as SOM, metal oxides/hydroxides, and clay minerals, play an important role in the photodegradation of anthracene.

SOM is a complex mixture of small and partially polymerized macromolecules (Lichtfouse, Chenu, et al., 1998; Lichtfouse, Leblond, et al., 1998), which controls the mobility and fate of PAHs. During photodegradation, SOM can either act as a photosensitizer to induce the generation of radicals that trigger the photodegradation of PAHs, or as quencher by competing with PAHs for oxidative radicals or electrons (Si, Zhou, et al., 2004; Fan et al., 2005).

On the one hand, SOM can enhance the photodegradation of PAHs as a photosensitizer. The enhancement can be attributed to the formation of SOM\* under light irradiation. Specifically, SOM possesses significant visible light absorption capacity, which can create reactive excited states, for example, SOM\*, after absorbing visible light (Wenk & Canonica, 2012). This excited SOM\* can transfer electrons to oxygen to produce ROS, which can enhance the indirect photodegradation of PAHs (Yap et al., 2011). On the other hand, the sequestration of PAHs in SOM reduces the photodegradation of PAHs, which is explained by less exposure to irradiation (Conte et al., 2001). In addition, the phenolic moieties in SOM are expected to provide electrons to ROS and  $\cdot\text{PAH}^+$ , thus quenching the indirect photolysis of PAHs (Lehto et al., 2003). Therefore, both promotion and inhibition of SOM on the photolysis of PAHs are likely to coexist in soils. The specific effects of SOM on the photolysis of PAHs may be explained by the difference of SOM fractions such as dissolved organic matter (DOM), humin (HM), humic acid (HA), and fulvic acid (FA), which have different functional groups, molecular weight, and redox sites. For example, Conte et al. (2001) reported that humin increases PAH retention in soils and decreases photodegradation of PAHs. By contrast, the photodegradation of PAHs is significantly enhanced by HA addition (Sun, Bai, et al., 2021). Similar to SOM, the organic amendments, such as biochar, have both positive and negative effects on the photodegradation of PAHs (Sun, Xiong, et al., 2021). Biochar can absorb light, and in turn induce the formation of ROS, which can then degrade PAHs. Contrastively, biochar can inhibit the photodegradation by reducing the photons available for photoreaction or scavenging the reactive oxidants.

Metal oxides/hydroxides, including  $\text{Fe}_2\text{O}_3$ ,  $\text{TiO}_2$ ,  $\text{ZnO}$ , and  $\text{FeOOH}$ , exhibit photocatalytic properties due to the electronic structure (Chakrabarti & Dutta, 2004; Soderstrom et al., 2004; Zhang, Li, et al., 2008). Among these metal oxides/hydroxides, iron (hydr)oxides occur widely in natural soils, and display an important role in photodegradation of PAHs (Marques et al., 2020; Yao et al., 2020). Various iron (hydr)oxides with different structures, for example, iron sulfides, magnetite ( $\gamma\text{-Fe}_2\text{O}_3$ ), goethite ( $\alpha\text{-FeOOH}$ ), hematite ( $\alpha\text{-Fe}_2\text{O}_3$ ), lepidocrocite ( $\gamma\text{-FeOOH}$ ), and green rust, have different photocatalytic effects on PAHs (Fu et al., 2005; Barzegar et al., 2017). For example, Wang et al. (2009) found that the photodegradation rate of pyrene on various types of iron oxides decreases in the order of  $\alpha\text{-FeOOH} > \alpha\text{-Fe}_2\text{O}_3 > \gamma\text{-Fe}_2\text{O}_3 > \gamma\text{-FeOOH}$ . Here, the higher activity of  $\alpha\text{-FeOOH}$  can be explained in two ways. On the one hand, the structure of morphology-acicular crystal makes  $\alpha\text{-FeOOH}$  containing higher inherent -OH groups on iron (hydr)oxide surfaces (Fe-OH), which can provide proper sites for  $\text{H}_2\text{O}_2$  to form H-bonds and facilitate the cleavage of O-O to produce more  $\cdot\text{OH}$ . On the other hand, the higher band gap of  $\alpha\text{-FeOOH}$  is easily excited to generate electron-hole pair after absorbing light, facilitating the formation of  $\cdot\text{OH}$ . The concentration of iron (hydr)oxides also influence the photodegradation of PAHs. Although the photocatalytic activity can be improved with a higher concentration of iron (hydr)oxides, the light utilization rate decreases with excessive dose (Wang et al., 2009). This is due to the decrease in light utilization caused by excessive iron (hydr)oxides. Therefore, it is important to optimize the dosage of iron (hydr)oxides for photodegradation of PAHs.

Other metal oxides such as anatase ( $\text{TiO}_2$ ) and aluminum oxide ( $\text{Al}_2\text{O}_3$ ) also act as photocatalysts for the degradation of PAHs in soils (Dong et al., 2010). For example, the photodegradation of phenanthrene and pyrene in soil is linearly enhanced by nanometer rutile  $\text{TiO}_2$  at 0 to 4 wt% under UV-light irradiation (Dong et al., 2010). Noteworthy, the photodegradation rate induced



by Fe<sub>2</sub>O<sub>3</sub>, TiO<sub>2</sub>, and ZnO decreases generally in the order: ZnO > TiO<sub>2</sub> > Fe<sub>2</sub>O<sub>3</sub>, because the band gap follows the order: ZnO (3.3 eV) > TiO<sub>2</sub> (3.2 eV) > Fe<sub>2</sub>O<sub>3</sub> (2.2 eV), and a larger band gap is beneficial for the photodegradation of PAHs. Besides, manganese oxides also promote the photodegradation of PAHs (Jokic et al., 2001; Jokic et al., 2004). MnO<sub>2</sub> is often used as a heterogeneous catalyst to accelerate the photolysis of PAHs due to its strong oxidizing capacity (Chien et al., 2011). One of the most widely occurring forms of manganese oxides is δ-MnO<sub>2</sub>, a short range ordered tetravalent Mn oxide (Wang et al., 2020). This type of Mn oxide is highly reactive in soils, promoting the efficient degradation of PAHs (Brunetti et al., 2008; Chien et al., 2011).

Quartz and clay minerals also influence the photodegradation of PAHs. The photodegradation of PAHs in quartz particles is explained by three phenomena: 1) the coarser and transparent texture of quartz is favoring light transmission; 2) the negligible organic matter content of quartz is beneficial to direct exposition PAHs to sunlight; and 3) the Lewis acid sites present on the quartz surface catalyze the oxidation of adsorbed PAHs (Dabestani et al., 1998; Chien et al., 2011). Besides quartz, various clay minerals play a major role in the photodegradation of PAHs (Zhu et al., 2004; Ciani et al., 2005; Dolly & Narahari, 2008). On the one hand, PAHs photolysis rates on cation-saturated clays depend on the cation exchange ability, which control the electron acceptor sites (Jia et al., 2012; Zhao et al., 2017). For example, photodegradation of phenanthrene decreases in the order Fe<sup>3+</sup>-smectite > Fe<sup>3+</sup>-vermiculite > Fe<sup>3+</sup>-kaolinite, in agreement with the order of exchangeable iron contents. On the other hand, the nature of cations on clays also influence the photolysis of PAHs. For instance, high charge-valences cations (i.e. Al<sup>3+</sup> and Fe<sup>3+</sup>) generally have strong polarizability and electron deficiency, which can facilitate electron transfer by providing strong bonding affinities for aromatic electron donor. Therefore, complexation with stronger interaction with transition metal ions is characterized by easier electron transfer and higher amount of ROS, facilitating the photodegradation of PAHs. In addition, the adsorption of PAHs on cation-modified clay mineral surface might alter PAHs spectral properties, and in turn the photolytic efficiency (Jia et al., 2015). For example, various spectral shifts are observed when anthracene is adsorbed on various cation-saturated clays (Anpo et al., 1990). The absorption band of anthracene on K<sup>+</sup>-smectite and Na<sup>+</sup>-smectite is red-shifted, which favors an efficient absorption of visible light and causes extended spectral overlap of PAHs and sunlight spectrum, resulting in enhanced photodegradation (Anpo et al., 1990; Jia et al., 2015). By contrast, a spectral shift is not observed in the reflectance spectrum when anthracene is adsorbed onto smectite saturated with Cu<sup>2+</sup>, Al<sup>3+</sup>, and Fe<sup>3+</sup>, and their spectral overlap with the emission spectrum of the visible light is negligible and have little effect on photodegradation (Jia et al., 2015).

The combined effects of SOM, metal oxides/hydroxides, and clay minerals also influence the photodegradation of PAHs (Dou et al., 2020). Various SOM fractions exhibit different behaviors in the photodegradation of PAHs on cation-modified clay minerals (Jia et al., 2013). The electron-donating ability of phenolic groups in DOM is higher than that of phenanthrene, which does not favor electron transfer of the phenanthrene, resulting a lower photodegradation rate of phenanthrene in Fe(III)-smectite. Contrastively, strong photosensitization and electrostatic interactions enhance the removal of phenanthrene following the addition of small amounts of FA and HA, whereas high content of HA and FA inhibits the removal of phenanthrene due to the quenching effect of SOM. Similar to SOM, various organic acids have different effects on the photodegradation of PAHs on cation-modified clay minerals. Organic acids, such as oxalic acid and malic acid, promote the photodegradation of phenanthrene via the generation of ·CO<sub>2</sub><sup>-</sup> radical (Jia et al., 2013). Organic acids can also reduce the photodegradation of PAHs because the number of effective sites on the clay surface is decreased (Elamamy & Mill, 1984). For example, oxalate, citric acid, and ethylene diamine tetraacetic acid, inhibit the photodegradation of PAHs on clay surfaces (Jia et al., 2014). This is due to the strong complexation between Fe(III) and organic ligands, which prevents PAHs from entering the metal ion sites and thus inhibit electron transfer. The combined effects of metal oxides/hydroxides and organic acids on the

photodegradation of PAHs are also ambiguous. On the one hand, the addition of oxalic acid promotes the photodegradation of PAHs by iron (hydr)oxides (Wang et al., 2009; Rani & Rachna, 2020). For example, Wang et al. (2009) reported that the combination of  $\alpha$ -FeOOH and oxalic acid can remove nine PAHs, with 12.2–21.8% removal efficiency, by a photo-Fenton-like reaction in a PAHs-contaminated soil. Here, the photodegradation rate of PAHs is not related to their molecular properties. On the other hand, oxalic acid, citric acid, tartaric acid and malic acid inhibit the degradation of PAHs via decreasing  $\cdot$ OH formation and occupying the active site of hematite, magnetite and goethite (Huang et al., 2019). The synergistic effect of metal oxides/hydroxides and clay minerals generally facilitates the photodegradation of PAHs. Mixtures of iron (hydr)oxides and clay minerals can enhance catalytic and photocatalytic activities (Nogueira et al., 2011; Vidal et al., 2015; Sun, Feng, et al., 2021). This is explained by the presence of more oxygen vacancies in the pillared structure of the mixture, and oxygen vacancies increase the generation of ROS under light. In the case of MnO<sub>2</sub>-supported clay, high oxidation potential and surface activity of hydroxyl structures facilitates the photodegradation of PAHs (Fang et al., 2016; He et al., 2018).

#### **2.4. Effects of soil environmental conditions**

The soil environmental conditions, such as layer thickness, particle size, temperature, oxygen content, pH, and water content, influence the photodegradation of PAHs. Generally, the photodegradation of PAHs mainly occurs in the thin layer of the soil surface (Zhang et al., 2006). When soil depth decreases from 4.0 to 1.0 mm, the half-life of benzo[a]pyrene decreases from 17.73 to 13.23 d, because a thinner soil layer facilitates the transmission of light and promotes photodegradation. Concerning soil particle size, the photodegradation rate is faster for coarse particles of 1 mm than for finer particles of 0.25 mm and 0.45 mm (Zhang et al., 2006). This is attributed by the fact that large particles are loosely packed, thus leaving more space for light scattering and permeating. Nonetheless, studies also found that low-molecular-weight and medium-molecular-weight PAHs undergo a higher photodegradation in fine-textured soil (Marques et al., 2017). In contrast, high-molecular-weight PAHs were more easily photodegraded in coarse-textured soil. Therefore, the effect of soil particle size on the photodegradation of PAHs needs further investigations.

Temperature significantly influence the photodegradation of PAHs in soils (Goss & Eisenreich, 1996). For instance, Coover and Sims (1987) found that increasing the temperature from 10 to 30 °C accelerated the photodegradation of PAHs by 5–79% in agricultural soils. Similarly, benzo[a]pyrene removal was increased by 20% when temperature increased from 20 to 30 °C (Zhang et al., 2006). The positive effects of higher temperatures on the photodegradation of PAHs is attributed to the higher solubility and vapor pressure of PAHs at higher temperatures (Balmer et al., 2000).

The photodegradation rate depends on the content of dioxygen (Jia et al., 2015). For instance, higher O<sub>2</sub> concentration increased the photodegradation rate of phenanthrene. This is explained by generation of ROS from O<sub>2</sub>, such as <sup>1</sup>O<sub>2</sub>, which promotes the photodegradation of PAHs. Photodegradation is also indirectly affected by pH because the the stability of iron species in soils is strongly dependent on pH (Jia et al., 2012). For instance, the photodegradation rate of phenanthrene in Fe(III)-smectite decreases when pH increases from 1.7 to 10.8. This is explained by the decrease of Fe<sup>3+</sup> content with pH, because Fe<sup>3+</sup> absorbs visible light and thus induces phenanthrene photodegradation.

The photodegradation of PAHs is affected by water content (Johnston et al., 2002; Jia et al., 2015). In Fe<sup>3+</sup>-smectite systems, the photodegradation rate of anthracene increased from 0.60 to 0.69 h<sup>-1</sup> as the relative humidity increased from ~ 0% to 38%, but further increase of the photodegradation rate was negligible above 56% relative humidity (Jia et al., 2015). The promotion effect of water on anthracene photodegradation can be ascribed to the generation of ROS, which

facilitate the degradation of anthracene (Wu et al., 2008; Zhang, Wu, et al., 2008). Nonetheless, anthracene degradation can be inhibited by water covering the surface of smectites because anthracene molecules are separated from the reactive cations by a water layer (Wu et al., 2008).

## 2.5. Products and pathways

The photodegradation of PAHs in soil is complex, and numerous intermediates have been detected. Table S1 presents the main products of photodegradation of anthracene, phenanthrene, pyrene, benzo[a]pyrene and chrysene. In general, products include complex mixtures of ketones, quinones, aldehydes, phenols and carboxylic acids (Rivas et al., 2000). Diones are often the initial major products. For instance, 9,10-anthracenedione was identified as the initial main product of anthracene (Jia et al., 2012). Further illumination yielded 1-hydroxy-9,10-anthracenedione, 1,4-dihydroxy-9,10-anthracenedione, 9-anthrone and 1(3H)-isobenzofuranone. Traces of phenanthrene-9,10-dione and 9,10-phenanthrenequinone were detected initially during the photodegradation of phenanthrene on clay mineral surfaces (Jia et al., 2012).

Benz[a]anthracene-7,12-dione and 1(3H)-isobenzofuranone were detected in the photodegradation of benz[a]anthracene (Lehto et al., 2003). Irradiation of dibenz[a,h]anthracene produced diones as initial products (Lehto et al., 2003). A 9-hydroxyfluorene was considered as the main photoproduct of fluorine, and benzo[a]pyrene-4,5-dihydrodiol and 2-hydroxy-benzo[a]pyrene-1,6-dione were detected during the degradation of benzo[a]pyrene (Dabrowska et al., 2008). Pyrenol was formed during the photolysis of pyrene on iron (hydr)oxides (Wang et al., 2009). Noteworthy, photodegradation of naphthalene, fluorene, anthracene and pyrene induced an increase of toxicity to aquatic microorganisms (Wang et al., 2009). This may be due to the production of photodegradation intermediates.

Environmentally persistent free radicals (EPFRs) were formed during the photodegradation of PAHs on metal-modified montmorillonite (Zhao et al., 2019; Jia, Zhao, Shi, Zhu, et al., 2019). EPFRs were also produced by photodegradation of anthracene in natural soils (Jia, Zhao, Shi, Fan, et al., 2019). EPFRs formed by photodegradation of PAHs usually have higher biological toxicity than parent compounds, since EPFRs can induce the formation of ROS, which are known to induce adverse effects on living organisms (Khachatryan et al., 2011). Therefore, the potential risk of products and intermediates during the photodegradation of PAHs should be investigated.

The general pathway of photodegradation of PAHs is shown in Figure 5. Photons can be either directly absorbed by PAHs molecules inducing the formation of PAH\* (Lehto et al., 2003); or photons can be first absorbed by a photosensitizer, such as SOM and black carbon, generating SOM\* and photoexcitation of surface oxygenated functional groups, respectively, which then transfer electrons to oxygen to produce ROS (Lehto et al., 2003). Due to their high reactivity, PAH\* are easily hydrolyzed by H<sub>2</sub>O/O<sub>2</sub>, generating intermediates such as hydroxylated PAHs,

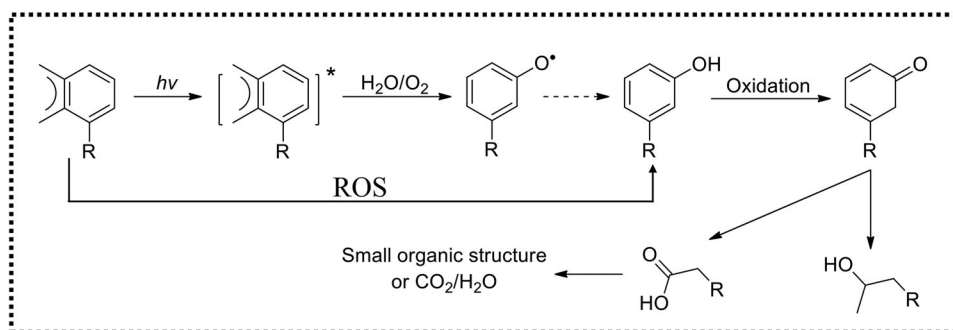


Figure 5. Proposed photodegradation pathway of polycyclic aromatic hydrocarbons (PAHs).

which are aromatic hydrocarbon receptors activators and developmental toxicants showing higher toxicity than parent PAHs (Wincent et al., 2015). Similarly, PAH can also be oxidized by ROS to generate hydroxylated PAHs. Hydroxylated PAHs are readily transformed to quinones (Miller & Olejnik, 2001). Quinones and hydroxylated PAHs are initial intermediates produced by addition of oxidative species such as oxygen and hydroxyl radicals (Miller & Olejnik, 2001). After that, intermediates undergo further oxidation and ring-opening to yield carboxylic acids (Szaciłowski et al., 2005). Finally, compounds of lower molecular weight such as alcohols are also produced and may be further degraded to CO<sub>2</sub> and H<sub>2</sub>O (Szaciłowski et al., 2005).

## 2.6. Current limitations

Overall, literature analysis shows that soil characteristics control the photodegradation of PAHs, with the highest photodegradation rates observed in soils with high content of metal oxides/hydroxides, clay minerals, and SOM. However, most studies have been conducted under ideal conditions in soil models containing few pure components. In the real soil environment, these components always co-exist as granular aggregate. The combined processes and internal mechanisms operating in natural soil systems are rarely clear due to their inherent complexity. There is therefore a need for studies in complex and natural systems.

## 3. Chemical oxidation of polycyclic aromatic hydrocarbons

Chemical oxidation plays a pivotal role in the transformation of PAHs in deep soil layers (Biache et al., 2011; Jia et al., 2015). Generally, the chemical oxidation of PAHs in soils proceeds by interfacial electron transfer and ROS (Kawahara et al., 2005; Liyanapatirana et al., 2010; Jia et al., 2016; Jia et al., 2020). Due to the differences in chemical oxidation mechanisms, chemical oxidation of PAHs is influenced by PAH properties, soil moieties, and soil environmental conditions (Biache et al., 2011; Li et al., 2015; Jia et al., 2015) (Figure 4).

### 3.1. Chemical oxidation mechanisms

On the one hand, electron transfer from PAHs to active sites on mineral surfaces contributes to PAHs transformation (Jia et al., 2016). Indeed, due to their highly delocalized  $\pi$ -electrons, PAHs act as electron donors when interacting with electron deficient species, for example, Lewis acid, on minerals (Kawahara et al., 2005). Such electron-donor-acceptor interactions induce electron transfer and the transformation of PAHs. Specifically, electron acceptor sites are associated with aluminum at crystal edges, and with transition metals on silicate layers, silica, and binary mineral systems such as SiO<sub>2</sub>/Al<sub>2</sub>O<sub>3</sub> and SiO<sub>2</sub>/TiO<sub>2</sub>, in soil phases (Dabestani et al., 1998). The combination of PAHs with electron-accepting sites induces the formation of a charge-transfer complex (Rooney & Pink, 1962; Kawahara et al., 2005). Then, an electron is initially transferred from a  $\pi$  orbital of adsorbed PAHs to the non-bound orbital, inducing the formation of cation- $\pi$  complexes on mineral surfaces. This decreases the electron density of PAHs and induces the generation of organic radical cations. The interaction between PAHs radical cations and charge accepting species, that is, H<sub>2</sub>O, induces the formation of PAH-quinones or PAH-hydroxyls and subsequent transformation of PAHs (Gu et al., 2008; Liyanapatirana et al., 2010)

On the other hand, PAHs can be oxidized by ROS, which are often generated in situ in soils. The generation of ROS is mediated by soil components such as inorganic minerals and humic substances. Concerning metal oxides/hydroxides, O<sub>2</sub> are first adsorbed by oxygen vacancies on metal oxides/hydroxides, then transformed into O<sub>2</sub><sup>-</sup>. In addition, the e<sub>g</sub><sup>1</sup> electrons in the anti-bonding of Mn<sup>3+</sup> of MnO<sub>2</sub> can be trapped by O<sub>2</sub>, and the generated Fe<sup>2+</sup> on Fe<sub>2</sub>O<sub>3</sub> can react with the adsorbed oxygen. All of these processes can induce the production of O<sub>2</sub><sup>-</sup>, facilitating

the transformation of PAHs (Wang et al., 2020; Ni et al., 2021). For SOM, the EPFRs in SOM can also induce the formation of ROS. Specifically, the electron transfers from EPFRs to  $O_2$  induces the generation of ROS, such as  $^1O_2$ ,  $O_2^-$ , and  $\cdot OH$ , thus promoting the transformation of PAHs (Jia et al., 2020).

### 3.2. Effects of PAH properties

The chemical oxidation of various PAHs in soils have been widely studied (Xu et al., 2018; Jia et al., 2016; Ni et al., 2021), and their disappearance kinetics and corresponding rate constants are compiled in Table S2. The oxidation of PAHs highly depends on their molecular properties, such as molar volume, dipole moment, energy highest occupied molecular orbital ( $E_{HOMO}$ ), energy lowest unoccupied molecular orbital ( $E_{LUMO}$ ), average polarizability, ionization potential (IP), electron affinity, and electrophilicity index (Jia et al., 2014; Jia et al., 2016; Xu et al., 2018). Generally, due to the nucleophilicity of PAHs, the IP controls the chemical oxidation of PAHs, and the reactivity increases with decreasing IP (Jia et al., 2014). For example, the transformation of various types of PAHs, including anthracene, pyrene, benzo[a]pyrene and phenanthrene, on Fe(III)-montmorillonite was 65, 90, 100 and  $\sim 0\%$ , respectively, under dehydrated conditions (Jia et al., 2014). This is explained by the different IP of PAHs. Indeed, electron transfer occurs easily for PAHs of lower IP, because these PAHs are easily oxidized to radical cations by nucleophilic reactions. By contrast, PAHs of higher IP withstand electron transfer, and this does not favor the oxidation of PAHs (Jia et al., 2016). In addition, lower IP is usually concomitant with higher  $E_{HOMO}$ , which are more reactive as a nucleophile (Xu et al., 2018). Thus, anthracene with  $E_{HOMO}$  of  $-5.6$  eV is more reactive than naphthalene with  $E_{HOMO}$  of  $-6.2$  eV, which is more reactive than benzene with  $E_{HOMO}$  of  $-7.2$  eV. More importantly, molecular properties such as dipole moment, electron affinity, and electrophilicity index, influence the IP and in turn PAHs transformation.

The effect of PAH molecular weight on PAH transformation is debated. On the one hand, the transformation rates of various PAHs on  $\alpha$ - $Fe_2O_3$  decreases with increasing molecular weight of naphthalene > anthracene > phenanthrene > benzo[a]pyrene (Ni et al., 2021). On the other hand, the transformation rates of PAHs on humin under redox conditions decreased with decreasing molecular weight of benzo[a]pyrene > anthracene > phenanthrene > naphthalene (Jia et al., 2020). This difference can be explained by different mechanisms of PAHs transformation. Indeed, both Fe(III) and  $O_2^-$  play an important role in the transformation of PAHs in the  $\alpha$ - $Fe_2O_3$  system, and are more readily to transform low-molecular-weight PAHs. For humin under redox conditions, the transformation of PAHs was mainly induced by ROS. ROS preferentially attacked tertiary carbon atoms of PAHs (Wang et al., 2019), and the transformation was related with the half-wave-potential ( $E_{1/2}$ ) of PAHs. The oxidative transformation was favorable for PAHs with low  $E_{1/2}$  values (Jia, Zhao, Shi, Fan, et al., 2019). Thus, the decay rate of benzo[a]pyrene ( $E_{1/2} = 0.94$ ) was higher than those of low-molecular-weight PAHs, i.e., anthracene ( $E_{1/2} = 1.09$ ), phenanthrene ( $E_{1/2} = 1.50$ ) and naphthalene ( $E_{1/2} = 1.70$ ).

### 3.3. Effects of soil moieties

The types of soil influence the chemical oxidation of PAHs (Jia, Zhao, Shi, Fan, et al., 2019). For instance, the chemical oxidation of anthracene in different types soils decreases in the order of red earth > yellow earth > latosol  $\sim$  fluvo-aquic soil > brown earth > chernozem > calcic brown soil (Jia, Zhao, Shi, Fan, et al., 2019). Compared with other types of soils, red earth, yellow earth, and latosols have higher content Fe and clay minerals. Chernozem possesses the highest content of organic carbon, followed by latosol and fluvo-aquic soils. Correlation analyses further shows that the chemical oxidation rate of anthracene is positive correlated with Fe, Mn and clay mineral

contents, and negative correlated with organic matter content. This suggests that the chemical oxidation of PAHs in soil depends on soil components.

In the absence of light, phenolic hydroxyl, carboxyl, quinone moieties within SOM are redox-active centers, which can oxidize PAHs directly (Zhang & Katayama, 2012). In addition, reduced natural organic matter can be oxidized by dioxygen under redox-dynamic environments conditions, contributing to  $\cdot\text{OH}$  production, then the formed  $\cdot\text{OH}$  can oxidize PAHs (Yuan et al., 2018). SOM can also mediate ROS production through indirect effects. Specifically, SOM can generate new EPFRs in response to changing of environmental conditions, for example, oxic/anoxic interfaces and flooding-drying cycling, and then induce the formation of ROS that can degrade PAHs (Jia et al., 2020). For example, treatment of humin with an oxidant, for example,  $\text{H}_2\text{O}_2$ , or reductant, for example, L-ascorbic acid, promotes the formation of newly reactive EPFRs, which are unstable and can induce the production of ROS, participating the transformation of PAHs (Jia et al., 2020). On the contrary, the retention, sorption, and sequestration of PAHs by SOM can reduce the chemical oxidation of PAHs (Chefetz et al., 2000; Rivas, 2006; Yang et al., 2010). Therefore, both promotion and inhibition of SOM on the transformation of PAHs are likely to coexist in soils, and the role and mechanism of SOM in the chemical oxidation of PAHs needs further investigation. In addition, organic/inorganic amendments, such as activated carbon, biochar, and minerals, have also been applied to the remediation of PAHs-contaminated soil due to their immobilization effect (Bolan et al., 2021).

Metal oxides/hydroxides also play an important role in the chemical oxidation of PAHs. Ni et al. (2021) recently found that  $\alpha\text{-Fe}_2\text{O}_3$ ,  $\text{Fe}_3\text{O}_4$ , and  $\alpha\text{-FeOOH}$  have a degrading effect on anthracene, and the transformation rate constants decrease in the order of  $\alpha\text{-Fe}_2\text{O}_3 > \text{Fe}_3\text{O}_4 > \alpha\text{-FeOOH}$ . This is due to the highest oxygen vacancy concentration on  $\alpha\text{-Fe}_2\text{O}_3$  that contributed to the exposure of Fe(III) and more active sites, promoting the transformation of anthracene. In addition, ROS generated by  $\text{Fe}_3\text{O}_4$  phase transition can oxidize PAHs (Yao et al., 2020). For example, the removal efficiency of  $\text{Fe}_3\text{O}_4$  for a PAHs-contaminated site (containing 13 types PAHs) is in the range of 37.7–85.2% (Barzegar et al., 2017). Notable, the removal efficiency of various PAH in contaminated soil is lower than that in anthropogenic single PAH-spiked soil. This can be attributed to a high pollution load caused by the presence of various aromatic and aliphatic hydrocarbons, which required higher doses of  $\text{Fe}_3\text{O}_4$  and longer reaction time. In particular, Fe(II)-bearing oxides, such as pyrite, siderite and magnetite, and Fe(II)-bearing clay minerals, such as nontronite and rectorite, are contributing to  $\cdot\text{OH}$  production upon redox-dynamic environments via a Fenton-like reaction, and the produced  $\cdot\text{OH}$  can oxidize PAHs (Zhang et al., 2016; Yuan et al., 2018).

The oxidative transformation of pyrene in the presence of  $\delta\text{-MnO}_2$  is also enhanced (Chien et al., 2011). Herein,  $\delta\text{-MnO}_2$  acts as a strong oxidizing agent with a very high reduction potential. The strong oxidative power of  $\delta\text{-MnO}_2$  to transform pyrene may be attributed to the layered structure within the tubular networks of  $\delta\text{-MnO}_2$  spheroids, which may result in a large area of inner specific surfaces that serve as electron acceptor sites. Noteworthy, Wang et al. (2020) recently reported that amorphous  $\text{MnO}_2$  displays higher catalytic activity than  $\alpha\text{-MnO}_2$ ,  $\beta\text{-MnO}_2$ ,  $\gamma\text{-MnO}_2$  and  $\delta\text{-MnO}_2$ , during the reaction with anthracene. This is due to the higher content of  $\text{Mn}^{3+}$  in amorphous  $\text{MnO}_2$ , which enhances the content of oxygen vacancies, promoting the level of  $\text{O}_2^-$ .

Clay minerals are generally recognized as one of the most chemically active components in soils, because clays act as catalysts in the oxidation of PAHs (Zhang et al., 1989; Trombetta et al., 2000; Si, Wang, et al., 2004; Ahn et al., 2006; Liu et al., 2011; Hanser et al., 2015). For example, a higher reactivity was observed during the oxidation of fluoranthene on limestone as compared to quartz (Ghislain et al., 2010). The transformation of PAHs in a clay system is also influenced by clay surface properties, such as cation hydration, location of charged layer, and types of ligands (Jia et al., 2014).

Smectite consists of a central octahedral Al-O sheet sandwiched between two tetrahedral Si-O sheets. Due to the isomorphic substitutions in tetrahedral Si and octahedral Al sheets, negative charges that are embedded in the individual layers in a fixed and isolated distribution are commonly neutralized by exchangeable hydrated cations in interlayer space (Gu et al., 2010). This unique property enables smectite to provide active sites for the adsorption and transformation of PAHs on mineral surfaces (Xiao et al., 2007; Tamamura et al., 2010; Zhang et al., 2011). PAHs are rich in delocalized  $\pi$  electrons and thus may interact strongly with electron-deficient or positively charged species via electron-donor-acceptor interactions (Qu et al., 2008). The formation of cation- $\pi$  interactions between  $\pi$  donor and exchangeable cations has been considered as a crucial factor affecting PAHs transformation (Gokel et al., 2001; Goss & Schwarzenbach, 2001; Qu et al., 2008).

Aluminosilicate can strongly adsorb  $O_2$  (Wang & Huang, 1989). Therefore,  $O_2$  molecules adsorbed and polarized by exposed structural cations on the edge sites of aluminosilicate play an important role in the ring cleavage of PAHs and the related reactions. The density and location of the active sites on aluminosilicate surface and crystal structure of aluminosilicate plays an important role in this process (Solomon, 1968). Moreover, the catalytic power of Al(III) on the edges and in the structure of nontronite was much higher than that of Al(III) on the edges of kaolinite and montmorillonite (Wang & Huang, 1989).

### **3.4. Effects of soil environmental conditions**

Soil environmental conditions, such as pH, moisture content, and temperature also influence the chemical oxidation of PAHs. Transformation is usually faster at low pH because low pH is generally associated with the higher contents of active Fe, which promotes the transformation of PAHs (Jia, Zhao, Shi, Fan, et al., 2019). In addition, Fe oxides can be activated at low pH, generating higher content of iron and favoring the transformation of PAHs (Jia, Zhao, Shi, Fan, et al., 2019). The effect of water on PAH oxidation is mainly due to the competition between water and PAHs for active sites (Karimi-Lotfabad et al., 1996). For example, the transformation of anthracene is slightly improved with moisture increasing from 8 to 11%, which is attributed to the fact that the ligand water molecules surrounding the exchangeable cation are involved in the reaction. Comparatively, the transformation rate is significantly decreased when the content of water exceeds 11% (Karimi-Lotfabad et al., 1996). This inhibitory effect is induced by the competition between PAHs and water for the access to Lewis acid sites on minerals (Rupert, 1973). Moreover, higher moisture induces more inhibition in soils with higher clay and iron minerals content, since the active sites or cations on mineral surfaces are likely to be hydrated, inducing the separation of PAHs from coordination sites and thus inhibiting the oxidation of PAHs (Qin et al., 2015; Jia, Zhao, Shi, Fan, et al., 2019). Specifically, the interaction of PAHs and inorganic minerals occurs mainly in reactive sites, which are likely to be hydrated under higher moisture, leading to the generation of water layer on mineral surfaces. The coverage of water molecules induces the separation of PAHs from the coordination sites such as Lewis acid sites (Qin et al., 2015).

Increasing the temperature accelerates the transformation rate of PAHs (Jia et al., 2016). This is due to the higher solubility and vapor pressure of PAHs at high temperatures (Balmer et al., 2000; Miller & Olejnik, 2001). The effect of  $O_2$  on the transformation of PAHs depends on PAH removal mechanisms in different systems. Compared with atmospheric condition, the degradation of anthracene is insignificantly influenced in real soils (relative anoxic condition), because soil minerals mediated oxidation plays a dominant role in the transformation of PAHs and is less affected by  $O_2$  (Jia, Zhao, Shi, Fan, et al., 2019). However, oxygen content can significantly affect the transformation of PAHs in humin under redox conditions because  $O_2$  determines the formation of ROS, which plays a critical role in the degradation of PAHs (Jia et al., 2020).

### 3.5. Products and pathways

The products of chemical oxidation of PAHs in soils are complex, and numerous intermediates have been detected. Table S2 presents the main products of anthracene, pyrene, fluoranthene, and benzo[a]pyrene.

Oxygenated PAHs are the main products of chemical oxidation of PAHs (Gao et al., 2018; Jia et al., 2020). Soil components can induce the formation of ROS, and in turn oxidize PAHs, mainly generating oxygenated PAHs (Wang et al., 2020; Ni et al., 2021). Similarly, electron transfer usually occurs between PAHs and clay minerals surfaces, leading to the generation of organic radicals, which are persistent in clay interlayers (Jia et al., 2016). Then organic radicals react with oxygenic species, inducing the generation of oxygenated products such as anthraquinone for anthracene, benzo[a]pyrene-6, 9-quinone for benzo[a]pyrene, and hydroxypyrene for pyrene (Joseph-Ezra et al., 2014; Jia et al., 2014). Those byproducts generally have higher aqueous solubility than their parent compounds, which may enhance the biological activity (Weigand et al., 2002). In addition, these products are usually toxic, mutagenic and carcinogenic, and therefore should be considered in the remediation of contaminated sites (Kazunga & Aitken, 2000).

More importantly, electron transfer from PAHs to electron deficient sites on clay surfaces can induce the generation of intermediate radicals (Roncovic et al., 2016). The intermediate radicals can be stabilized on clay surfaces and produce EPFRs, which may induce adverse effects on living organisms (Jia et al., 2016). For example, Jia et al. (2016) observed the formation of EPFRs during anthracene interaction with Fe(III)-modified clays. Jia et al. (2017) also characterized the distribution and stabilization of EPFRs in soils contaminated by PAHs and proposed that EPFRs are often involved in the transformation of PAHs (Jia et al., 2018). In addition, Zhao et al. (2019) reported that the interaction of benzo[a]pyrene with Cu(II)-montmorillonite can produce EPFRs and ROS, causing a negative effect on the growth of human gastric epithelial GES-1 cells.

To conclude, various soil moieties have different effects on PAHs transformation products. EPFRs are generated in the transformation of PAHs on clay minerals, rather than on metal oxides/hydroxides (Jia et al., 2018). This may be due to the protective effect of clay minerals on free radical intermediates, inducing the formation of EPFRs. In addition, metal oxides/hydroxides can form ROS, which alter the structure of PAHs and its intermediates, promoting ring opening and mineralization (Wang et al., 2020). However, the transformation of PAHs on clay minerals is only a process of electron transfer, forming quinone-based PAHs that cannot be further transformed (Jia et al., 2018; Jia, Zhao, Shi, Zhu, et al., 2019).

### 3.6. Current limitations

Overall, chemical oxidation, which refers to the direct redox actions between soil components and contaminants under ambient conditions, plays a pivotal role in dissipating PAHs. However, due to the lack of external energy, it usually takes a long time to achieve the complete removal of PAHs. The practical application of chemical oxidation is significantly influenced by soil active components, which are composited by SOM, clay minerals and metal oxides/hydroxides. Nonetheless, the controlling factors for the in-situ formation of active components are still unclear. Therefore, the efficiency of chemical oxidation associated with active components needs further investigation.

## 4. Applications of abiotic transformation

The abundance and properties of microorganisms, and the mass load and types of active components dominate the contribution of biodegradation and abiotic transformation of a site, respectively (Butler et al., 2013). Under favorable conditions, abiotic processes play an important role in



the natural attenuation. For instance, abiotic processes accounted for 11.8–99.7% of PAHs disappearance in coking soil and 30.7–68.6% of anthracene dissipation in anthropic anthracene-spiked cultivated soils (Liu et al., 2021). Authors also observed that abiotic attenuation played a significant role when the soil contained high levels of transition metals, such as Fe, Cu and Mn (Jia et al., 2018; Liu et al., 2021). Photodegradation is the most important abiotic process for the degradation of PAHs in soil surface layer, and chemical oxidation plays a pivotal role in the degradation of PAHs in deep soil layers. Both of them determine the application of abiotic transformation. The following directions should be considered for the practical application of photodegradation and chemical oxidation:

- developing novel photocatalysts that not only promote the photocatalytic degradation, but also enhance the adsorption of reactants;
- building photoreactor systems that can upgrade the transfer of photon, the distribution and use of light, and prepare for scale-up;
- developing organic carbon, metal oxides/hydroxides and clay minerals-based materials for in-situ remediation of PAHs-contaminated soils;
- designing a chemical oxidation system that can work efficiently to degrade PAHs in less time.

Overall, the practical application of abiotic transformation engineering is significantly influenced by the natural geochemical conditions, especially active components, in a field. Understanding of the main controlling factors for the formation of active components can stimulate their formation by manipulating geochemical conditions, which can promote abiotic transformation of PAHs, and is critical for designing and implementing abiotic remediation engineering.

## 5. Conclusions and prospects

In this review, photodegradation and chemical oxidation in abiotic transformation of PAHs, such as reactivity, products, pathways, and mechanism, were summarized in detail. The significant effects of soil components, including SOM, metal oxides/hydroxides, and clay minerals, for abiotic transformation of PAHs were also systematically investigated. Overall, abiotic transformation of PAHs occurs easily when PAHs match better the solar spectrum and are prone to transfer electron, when soil contains more active components (e.g. SOM, metal oxides/hydroxides, and clay minerals), when the bond energy between soil components and PAHs molecules is strong, and when soil environmental conditions favor sunlight absorption or/and ROS production.

Based on the current knowledge and latest progress in the field, the following research guidelines are suggested:

1. Developing identification and quantification methods of active minerals in field samples, this can provide preconditions for the application of abiotic transformation in PAHs contaminated soil.
2. Connecting laboratory batch research rates with field conditions, and determining the methods to increase rates in laboratory experiments and field applications. There is an urgent need to apply the laboratory to the field site, realizing the up-scale and integrated remediation of PAHs-contaminated soil.
3. The chemical reactivity of breakdown products is significant for risk assessment of PAHs in soils. Both photodegradation and chemical oxidation of PAHs can produce EPFRs. Identifying such reactive chemicals and testing the toxicity of those products will provide a theoretical basis for the safe and effective application of abiotic transformation technology.

4. Abiotic transformation of PAHs usually produces oxygenated PAHs with higher solubility, which may enhance the biological activity. However, there is currently no systematic understanding of the impact of abiotic transformation on biodegradation. Further investigations are needed to clearly clarify this issue.

## Disclosure statement

The authors declare that they have no known competing financial interests or personal relationships that could have appeared to influence the work reported in this paper.

## Funding

This study was supported by the National Key R&D Program of China (Grant No. 2018YFC1802004), the National Natural Science Foundation of China (Grant No. 41877126), the Shaanxi Science Fund for Distinguished Young Scholars (Grant No. 2019JC-18), and the “One Hundred Talents” program of Shaanxi Province (Grant No. SXBR9171).

## References

- Ahn, M.-Y., Filley, T. R., Jafvert, C. T., Nies, L., Hua, I., & Bezares-Cruz, J. (2006). Photodegradation of decabromodiphenyl ether adsorbed onto clay minerals, metal oxides, and sediment. *Environmental Science & Technology*, *40*(1), 215–220. <https://doi.org/10.1021/es051415t>
- Alegbeleye, O. O., Opeolu, B. O., & Jackson, V. A. (2017). Polycyclic aromatic hydrocarbons: a critical review of environmental occurrence and bioremediation. *Environmental Management*, *60*(4), 758–783. <https://doi.org/10.1007/s00267-017-0896-2>
- Anpo, M., Nishiguchi, H., & Fujii, T. (1990). Photophysics and photochemistry in the adsorbed layer: Effects of solid surfaces upon the excited states and the photoreactions of adsorbed molecules. *Research on Chemical Intermediates*, *13*(1), 73–102. <https://doi.org/10.1163/156856790X00076>
- Barzegar, G., Jorfi, S., Soltani, R. D. C., Ahmadi, M., Saeedi, R., Abtahi, M., Ramavandi, B., & Baboli, Z. (2017). Enhanced sono-Fenton-like oxidation of PAH-contaminated soil using nano-sized magnetite as catalyst: optimization with response surface methodology. *Soil and Sediment Contamination: An International Journal*, *26*(5), 538–557. <https://doi.org/10.1080/15320383.2017.1363157>
- Bolan, N., Sarkar, B., Vithanage, M., Singh, G., Tsang, D. C. W., Mukhopadhyay, R., Ramadass, K., Vinu, A., Sun, Y. Q., Ramanayaka, S., Hoang, S. A., Yan, Y. B., Li, Y., Rinklebe, J., Li, H., & Kirkham, M. B. (2021). Distribution, behaviour, bioavailability and remediation of poly- and per-fluoroalkyl substances (PFAS) in solid biowastes and biowaste-treated soil. *Environment International*, *155*, 106600. <https://doi.org/10.1016/j.envint.2021.106600>
- Balmer, M. E., Goss, K., & Schwarzenbach, R. P. (2000). Photolytic transformation of organic pollutants on soil surfaces—an experimental approach. *Environmental Science & Technology*, *34*(7), 1240–1245. <https://doi.org/10.1021/es990910k>
- Biache, C., Faure, P., Mansuy-Huault, L., Cébron, A., Beguiristain, T., & Leyval, C. (2013). Biodegradation of the organic matter in a coking plant soil and its main constituents. *Organic Geochemistry*, *56*, 10–18. <https://doi.org/10.1016/j.orggeochem.2012.12.002>
- Biache, C., Ghislain, T., Faure, P., & Mansuy-Huault, L. (2011). Low temperature oxidation of a coking plant soil organic matter and its major constituents: An experimental approach to simulate a long term evolution. *Journal of Hazardous Materials*, *188*(1-3), 221–230. <https://doi.org/10.1016/j.jhazmat.2011.01.102>
- Biache, C., Mansuy-Huault, L., & Faure, P. (2014). Impact of oxidation and biodegradation on the most commonly used polycyclic aromatic hydrocarbon (PAH) diagnostic ratios: Implications for the source identifications. *Journal of Hazardous Materials*, *267*, 31–39. <https://doi.org/10.1016/j.jhazmat.2013.12.036>
- Brunetti, G., Senesi, N., & Plaza, C. (2008). Organic matter humification in olive oil mill wastewater by abiotic catalysis with manganese(IV) oxide. *Bioresource Technology*, *99*(17), 8528–8531. <https://doi.org/10.1016/j.biortech.2008.02.047>
- Bryselbout, C., Henner, P., Carsignol, J., & Lichtfouse, E. (2000). Polycyclic aromatic hydrocarbons in highway plants and soils: Evidence for a local distillation effect. *Analisis* *28*(4), 290–293. <https://doi.org/10.1051/analisis:2000280290>

- Butler, E. C., Chen, L., & Darlington, R. (2013). Transformation of trichloroethylene to predominantly non-regulated products under stimulated sulfate reducing conditions. *Groundwater Monitoring & Remediation*, 33(3), 52–60. <https://doi.org/10.1111/gwmr.12015>
- Butler, E. C., & Hayes, K. F. (2000). Kinetics of the transformation of halogenated aliphatic compounds by iron sulfide. *Environmental Science & Technology*, 34(3), 422–429. <https://doi.org/10.1021/es980946x>
- Cavoski, I., Caboni, P., Sarais, G., Cabras, P., & Miano, T. M. (2007). Photodegradation of rotenone in soils under environmental conditions. *Journal of Agricultural and Food Chemistry*, 55(17), 7069–7074. <https://doi.org/10.1021/jf0708239>
- Chakrabarti, S., & Dutta, B. K. (2004). Photocatalytic degradation of model textile dyes in wastewater using ZnO as semiconductor catalyst. *Journal of Hazardous Materials*, 112(3), 269–278. <https://doi.org/10.1016/j.jhazmat.2004.05.013>
- Chefetz, B., Deshmukh, P. A., Hatcher, P. G., & Guthrie, E. A. (2000). Pyrene sorption by natural organic matter. *Environmental Science & Technology*, 34(14), 2925–2930. <https://doi.org/10.1021/es9912877>
- Cheng, C., Lehmann, J., Thies, J. E., Burton, S. D., & Engelhard, M. H. (2006). Oxidation of black carbon by biotic and abiotic processes. *Organic Geochemistry*, 37(11), 1477–1488. <https://doi.org/10.1016/j.orggeochem.2006.06.022>
- Chien, S. W. C., Chang, C. H., Chen, S. H., Wang, M. C., Rao, M. M., & Veni, S. S. (2011). Oxidative degradation of pyrene in contaminated soils by  $\delta$ -MnO<sub>2</sub> with or without sunlight irradiation. *The Science of the Total Environment*, 409(19), 4078–4086. <https://doi.org/10.1016/j.scitotenv.2011.06.019>
- Ciani, A., Goss, K., & Schwarzenbach, R. P. (2005). Light penetration in soil and particulate minerals. *European Journal of Soil Science*, 56(5), 561–574. <https://doi.org/10.1111/j.1365-2389.2005.00688.x>
- Conte, P., Zena, A., Pilidis, G., & Piccolo, A. (2001). Increased retention of polycyclic aromatic hydrocarbons in soils induced by soil treatment with humic substances. *Environmental Pollution (Barking, Essex : 1987)*, 112(1), 27–31. [https://doi.org/10.1016/S0269-7491\(00\)00101-9](https://doi.org/10.1016/S0269-7491(00)00101-9)
- Coover, M. P., & Sims, R. C. (1987). The effect of temperature on polycyclic aromatic hydrocarbon persistence in an unacclimated agricultural soil. *Hazardous Waste and Hazardous Materials*, 4(1), 69–82. <https://doi.org/10.1089/hwm.1987.4.69>
- Dabestani, R., Reszka, K. J., & Sigman, M. E. (1998). Surface catalyzed electron transfer from polycyclic aromatic hydrocarbons (PAH) to methyl viologen dication: evidence for ground-state charge transfer complex formation on silica gel. *Journal of Photochemistry and Photobiology A: Chemistry*, 117(3), 223–233. [https://doi.org/10.1016/S1010-6030\(98\)00327-X](https://doi.org/10.1016/S1010-6030(98)00327-X)
- Dabrowska, D., Kotwasik, A., & Namiesnik, J. (2008). Stability studies of selected polycyclic aromatic hydrocarbons in different organic solvents and identification of their transformation products. *Polish Journal of Environmental Studies*, 17, 17–24.
- Dolly, V., & Narahari, S. G. (2008). Exploring the size dependence of cyclic and acyclic pi-systems on cation-pi binding. *Physical Chemistry Chemical Physics*, 10, 582–590.
- Dong, D. B., Li, P. J., Li, X. J., Xu, C. B., Gong, D. W., Zhang, Y. Q., Zhao, Q., & Li, P. (2010). Photocatalytic degradation of phenanthrene and pyrene on soil surfaces in the presence of nanometer rutile TiO<sub>2</sub> under UV-irradiation. *Chemical Engineering Journal*, 158(3), 378–383. <https://doi.org/10.1016/j.cej.2009.12.046>
- Dong, Y. R., Liang, X. M., Krumholz, L. R., Philp, R. P., & Butler, E. C. (2009). The relative contributions of abiotic and microbial processes to the transformation of tetrachloroethylene and trichloroethylene in anaerobic microcosms. *Environmental Science & Technology*, 43(3), 690–697. <https://doi.org/10.1021/es801917p>
- Dou, S., Shan, J., Song, X. Y., Cao, R., Meng, W. U., Li, C. L., & Song, G. (2020). Are humic substances soil microbial residues or unique synthesized compounds? A perspective on their distinctiveness. *Pedosphere* 30(2), 159–167. [https://doi.org/10.1016/S1002-0160\(20\)60001-7](https://doi.org/10.1016/S1002-0160(20)60001-7)
- Duan, Y. H., Shen, G. F., Tao, S., Hong, J. P., Chen, Y. C., Xue, M., Li, T. C., Su, S., Shen, H. Z., Fu, X. F., Meng, Q. C., Zhang, J., Zhang, B., Han, X. Y., & Song, K. (2015). Characteristics of polycyclic aromatic hydrocarbons in agricultural soils at a typical coke production base in Shanxi, China. *Chemosphere* 127, 64–69. <https://doi.org/10.1016/j.chemosphere.2014.12.075>
- Elamamy, M. M., & Mill, T. (1984). Hydrolysis kinetics of organic chemicals on montmorillonite and kaolinite surfaces as related to moisture content. *Clays and Clay Minerals*, 32, 67–73.
- Eriksson, M., Dalhammar, G., & Borg-Karlson, A. K. (2000). Biological degradation of selected hydrocarbons in an old PAH/creosote contaminated soil from a gas work site. *Applied Microbiology and Biotechnology*, 53(5), 619–626. <https://doi.org/10.1007/s002530051667>
- Fang, L., Hong, R., Gao, J., & Gu, C. (2016). Degradation of bisphenol A by nano-sized manganese dioxide synthesized using montmorillonite as templates. *Applied Clay Science*, 132–133, 155–160. <https://doi.org/10.1016/j.clay.2016.05.028>
- Fan, X. Z., Lu, B., & Gong, A. J. (2005). Dynamics of solar light photodegradation behavior of atrazine on soil surface. *Journal of Hazardous Materials*, 117, 75–79.

- Fox, M. A., & Olive, S. (1979). Photooxidation of anthracene on atmospheric particulate matter. *Science (New York, N.Y.)*, 205(4406), 582–583. <https://doi.org/10.1126/science.205.4406.582>
- Fu, H. B., Xie, Q., & Zhao, H. M. (2005). Photodegradation of  $\gamma$ -HCH by  $\alpha$ -Fe<sub>2</sub>O<sub>3</sub> and the influence of fulvic acid. *Journal of Photochemistry and Photobiology A: Chemistry*, 173(2), 143–149. <https://doi.org/10.1016/j.jphotochem.2005.01.013>
- Gokel, G. W., Barbour, L. J., De-Wall, S. L., & Meadows, E. S. (2001). Macrocyclic polyethers as probes to assess and understand alkali metal cation- $\pi$  interactions. *Coordination Chemistry Reviews*, 222(1), 127–154. [https://doi.org/10.1016/S0010-8545\(01\)00380-0](https://doi.org/10.1016/S0010-8545(01)00380-0)
- Ghislain, T., Faure, P., Biache, C., & Michels, R. (2010). Low-temperature, mineral-catalyzed air oxidation: a possible new pathway for pah stabilization in sediments and soils. *Environmental Science & Technology*, 44(22), 8547–8552. <https://doi.org/10.1021/es102832r>
- Goss, K., & Eisenreich, S. J. (1996). Adsorption of VOCs from the gas phase to different minerals and a mineral mixture. *Environmental Science & Technology*, 30(7), 2135–2142. <https://doi.org/10.1021/es950508f>
- Goss, K., & Schwarzenbach, R. P. (2001). Linear free energy relationships used to evaluate equilibrium partitioning of organic compounds. *Environmental Science & Technology*, 35(1), 1–9. <https://doi.org/10.1021/es000996d>
- Grova, N., Laurent, C., Feidt, C., Rychen, G., Laurent, F., & Lichtfouse, E. (2000). Gas chromatography-mass spectrometry study of polycyclic aromatic hydrocarbons in grass and milk from urban and rural farms. *European Journal of Mass Spectrometry*, 6(5), 457–460. <https://doi.org/10.1255/ejms.371>
- Gu, C., Jia, H., Li, H., Teppen, B. J., & Boyd, S. A. (2010). Synthesis of highly reactive subnano-sized zero-valent iron using smectite clay templates. *Environmental Science & Technology*, 44(11), 4258–4263. <https://doi.org/10.1021/es903801r>
- Gu, C., Li, H., Teppen, B. J., & Boyd, S. A. (2008). Octachlorodibenzodioxin formation on Fe(III)-montmorillonite clay. *Environmental Science & Technology*, 42(13), 4758–4763. <https://doi.org/10.1021/es7029834>
- Gao, P., Yao, D. C., Qian, Y. J., Zhong, S., Zhang, L. S., Xue, G., & Jia, H. Z. (2018). Factors controlling the formation of persistent free radicals in hydrochar during hydrothermal conversion of rice straw. *Environmental Chemistry Letters*, 16(4), 1463–1468. <https://doi.org/10.1007/s10311-018-0757-0>
- Huang, D., Wang, T. C., Zhu, K. C., Zhao, S., Shi, Y. F., Ye, M., Wang, C. Y., & Jia, H. Z. (2019). Low-molecular-weight organic acids impede the degradation of naphthol in iron oxides/persulfate systems: Implications for research experiments in pure conditions. *Chemosphere* 225, 1–8. <https://doi.org/10.1016/j.chemosphere.2019.02.127>
- He, Y., Jiang, D., Chen, J., Jiang, D. Y., & Zhang, Y. X. (2018). Synthesis of MnO<sub>2</sub> nanosheets on montmorillonite for oxidative degradation and adsorption of methylene blue. *Journal of Colloid and Interface Science*, 510, 207–220. <https://doi.org/10.1016/j.jcis.2017.09.066>
- Hanser, O., Biache, C., Boulange, M., Parant, S., Lorgeoux, C., Billet, D., Michels, R., & Faure, P. (2015). Evolution of dissolved organic matter during abiotic oxidation of coal tar-comparison with contaminated soils under natural attenuation. *Environmental Science and Pollution Research International*, 22(2), 1431–1443. <https://doi.org/10.1007/s11356-014-3465-8>
- Haritash, A. K., & Kaushik, C. P. (2009). Biodegradation aspects of polycyclic aromatic hydrocarbons (PAHs): A review. *Journal of Hazardous Materials*, 169(1-3), 1–15. <https://doi.org/10.1016/j.jhazmat.2009.03.137>
- Harvey, P. J., Campanella, B. F., Castro, P. M. L., Harms, H., Lichtfouse, E., Schaffner, A. R., Smrcek, S., & Werck-Reichhart, D. (2002). Phytoremediation of polyaromatic hydrocarbons, anilines and phenols. *Environmental Science and Pollution Research International*, 9(1), 29–47. <https://doi.org/10.1007/BF02987315>
- Huber, S., Wunderlich, S., Scholer, H. F., & Williams, J. (2010). Natural abiotic formation of furans in soil. *Environmental Science & Technology*, 44(15), 5799–5804. <https://doi.org/10.1021/es100704g>
- Jia, H. Z., Zhao, S., Shi, Y. F., Zhu, K. C., Gao, P., & Zhu, L. Y. (2019). Mechanisms for light-driven evolution of environmentally persistent free radicals and photolytic degradation of PAHs on Fe(III)-montmorillonite surface. *Journal of Hazardous Materials*, 362, 92–98. <https://doi.org/10.1016/j.jhazmat.2018.09.019>
- Jia, H. Z., Zhao, S., Shi, Y. F., Fan, X. Y., & Wang, T. C. (2019). Formation of environmentally persistent free radicals during the transformation of anthracene in different soils: Roles of soil characteristics and ambient conditions. *Journal of Hazardous Materials*, 362, 214–223. <https://doi.org/10.1016/j.jhazmat.2018.08.056>
- Jia, H. Z., Zhao, S., Shi, Y. F., Zhu, L. Y., Wang, C. Y., & Sharma, V. K. (2018). Transformation of polycyclic aromatic hydrocarbons and formation of environmentally persistent free radicals on modified montmorillonite: The role of surface metal ions and polycyclic aromatic hydrocarbon molecular properties. *Environmental Science & Technology*, 52(10), 5725–5733. <https://doi.org/10.1021/acs.est.8b00425>
- Jia, H. Z., Li, L., Chen, H. X., Zhao, Y., Li, X. Y., & Wang, C. Y. (2015). Exchangeable cations-mediated photodegradation of polycyclic aromatic hydrocarbons (PAHs) on smectite surface under visible light. *Journal of Hazardous Materials*, 287, 16–23. <https://doi.org/10.1016/j.jhazmat.2015.01.040>
- Jia, H. Z., Li, L., Fan, X. Y., Liu, M. D., Deng, W. Y., & Wang, C. Y. (2013). Visible light photodegradation of phenanthrene catalyzed by Fe(III)-smectite: role of soil organic matter. *Journal of Hazardous Materials*, 256-257, 16–23. <https://doi.org/10.1016/j.jhazmat.2013.04.014>

- Jia, H. Z., Nulaji, G., Gao, H. W., Wang, F., Zhu, Y. Q., & Wang, C. Y. (2016). Formation and stabilization of environmentally persistent free radicals induced by the interaction of anthracene with Fe(III)-modified clays. *Environmental Science & Technology*, 50(12), 6310–6319. <https://doi.org/10.1021/acs.est.6b00527>
- Jia, H. Z., Shi, Y. F., Nie, X. F., Zhao, S., Wang, T. C., & Sharma, V. K. (2020). Persistent free radicals in humin under redox conditions and their impact in transforming polycyclic aromatic hydrocarbons. *Frontiers of Environmental Science & Engineering*, 14(4), 73–83.
- Jia, H. Z., Zhao, J. C., Fan, X. Y., Dilimulati, K., & Wang, C. Y. (2012). Photodegradation of phenanthrene on cation-modified clays under visible light. *Applied Catalysis B: Environmental*, 123–124, 43–51. <https://doi.org/10.1016/j.apcatb.2012.04.017>
- Jia, H. Z., Zhao, J. C., Li, L., Li, X. Y., & Wang, C. Y. (2014). Transformation of polycyclic aromatic hydrocarbons (PAHs) on Fe(III)-modified clay minerals: Role of molecular chemistry and clay surface properties. *Applied Catalysis B: Environmental*, 154–155, 238–245. <https://doi.org/10.1016/j.apcatb.2014.02.022>
- Jia, H. Z., Zhao, S., Nulaji, G., Tao, K. L., Wang, F., Sharma, V. K., & Wang, C. Y. (2017). Environmentally persistent free radicals in soils of past coking sites: distribution and stabilization. *Environmental Science & Technology*, 51(11), 6000–6008. <https://doi.org/10.1021/acs.est.7b00599>
- Johnston, C. T., Sheng, G., Teppen, B. J., Boyd, S. A., & De-Oliveira, M. F. (2002). Spectroscopic study of dinitrophenol herbicide sorption on smectite. *Environmental Science & Technology*, 36(23), 5067–5074. <https://doi.org/10.1021/es025760j>
- Jokic, A., Frenkel, A. I., Vairavamurthy, M. A., & Huang, P. M. (2001). Birnessite catalysis of the maillard reaction: Its significance in natural humification. *Geophysical Research Letters*, 28(20), 3899–3902. <https://doi.org/10.1029/2001GL013839>
- Jokic, A., Wang, M. C., Liu, C., Frenkel, A. I., & Huang, P. M. (2004). Integration of the polyphenol and Maillard reactions into a unified abiotic pathway for humification in nature: the role of  $\delta$ -MnO<sub>2</sub>. *Organic Geochemistry*, 35, 0–762.
- Joseph-Ezra, H., Nasser, A., & Mingelgrin, U. (2014). Surface interactions of pyrene and phenanthrene on Cu-montmorillonite. *Applied Clay Science*, 95, 348–356. <https://doi.org/10.1016/j.clay.2014.04.037>
- Kanally, R. A., & Harayama, S. (2000). Biodegradation of high-molecular-weight polycyclic aromatic hydrocarbons by bacteria. *Journal of Bacteriology*, 182(8), 2059–2067. <https://doi.org/10.1128/JB.182.8.2059-2067.2000>
- Karimi-Lotfabad, S., Pickard, M. A., & Gray, M. R. (1996). Reactions of polynuclear aromatic hydrocarbons on soil. *Environmental Science & Technology*, 30(4), 1145–1151. <https://doi.org/10.1021/es950365x>
- Katagi, T. (1990). Photoinduced oxidation of the organophosphorus fungicide tolclofos-methyl on clay minerals. *Journal of Agricultural and Food Chemistry*, 38(7), 1595–1600. <https://doi.org/10.1021/jf00097a035>
- Kawahara, S. C., Tsuzuki, S., & Uchimar, T. (2005). Lewis acidity/basicity of pi-electron systems: theoretical study of a molecular interaction between a pi system and a Lewis acid/base. *Chemistry (Weinheim an der Bergstrasse, Germany)*, 11(15), 4458–4464. <https://doi.org/10.1002/chem.200400912>
- Kazunga, C., & Aitken, M. D. (2000). Products from the incomplete metabolism of pyrene by polycyclic aromatic hydrocarbon-degrading bacteria. *Applied and Environmental Microbiology*, 66(5), 1917–1922. <https://doi.org/10.1128/AEM.66.5.1917-1922.2000>
- Khachatryan, L., Vejerano, E. P., Lomnicki, S., & Dellinger, B. (2011). Environmentally persistent free radicals (EPFRs). I. Generation of reactive oxygen species in aqueous solutions. *Environmental Science & Technology*, 45(19), 8559–8566. <https://doi.org/10.1021/es201309c>
- Kong, L., & Ferry, J. L. (2003). Effect of salinity on the photolysis of chrysene adsorbed to a smectite clay. *Environmental Science & Technology*, 37(21), 4894–4900. <https://doi.org/10.1021/es026124o>
- Lehner, A. F., Horn, J., & Flesher, J. W. (2004). Formation of radical cations in a model for the metabolism of aromatic hydrocarbons. *Biochemical and Biophysical Research Communications*, 322(3), 1018–1023. <https://doi.org/10.1016/j.bbrc.2004.08.017>
- Lehto, K., Puhakka, J. A., & Lemmetyinen, H. (2003). Photodegradation products of polycyclic aromatic hydrocarbons in water and their amenability to biodegradation. *Polycyclic Aromatic Compounds*, 23(4), 401–416. <https://doi.org/10.1080/713743538>
- Li, L., Jia, H. Z., Li, X. Y., & Wang, C. Y. (2015). Transformation of anthracene on various cation-modified clay minerals. *Environmental Science and Pollution Research International*, 22(2), 1261–1269. <https://doi.org/10.1007/s11356-014-3424-4>
- Lichtfouse, E., Budzinski, H., Garrigues, P., & Eglinton, T. I. (1997). Ancient polycyclic aromatic hydrocarbons in modern soils: <sup>13</sup>C, <sup>14</sup>C and biomarker evidence. *Organic Geochemistry*, 26(5–6), 353–359. [https://doi.org/10.1016/S0146-6380\(97\)00009-0](https://doi.org/10.1016/S0146-6380(97)00009-0)
- Lichtfouse, E., Chenu, C., Baudin, F., Leblond, C., Silva, M. D., Behar, F., Derenne, S., Largeau, C., Wehrung, P., & Albrecht, P. (1998). A novel pathway of soil organic matter formation by selective preservation of resistant straight-chain biopolymers: Chemical and isotope evidence. *Organic Geochemistry*, 28(6), 411–415. [https://doi.org/10.1016/S0146-6380\(98\)00005-9](https://doi.org/10.1016/S0146-6380(98)00005-9)

- Lichtfouse, E., Leblond, C., Silva, M. D., & Behar, F. (1998). Occurrence of biomarkers and straight-chain biopolymers in humin: Implication for the origin of soil organic matter. *Naturwissenschaften*, 85(10), 497–501. <https://doi.org/10.1007/s001140050538>
- Liu, J. B., Zhao, S., Zhang, R., Dai, Y. C., Zhang, C., Jia, H. Z., & Guo, X. T. (2021). How important is abiotic dissipation in natural attenuation of polycyclic aromatic hydrocarbons in soil? *The Science of the Total Environment*, 758, 143687. <https://doi.org/10.1016/j.scitotenv.2020.143687>
- Liu, Y. X., Lu, X. J., Wu, F., & Deng, N. S. (2011). Adsorption and photooxidation of pharmaceuticals and personal care products on clay minerals. *Reaction Kinetics, Mechanisms and Catalysis*, 104(1), 61–73. <https://doi.org/10.1007/s11144-011-0349-5>
- Liyanapatirana, C., Gwaltney, S. R., & Xia, K. (2010). Transformation of triclosan by Fe(III)-saturated montmorillonite. *Environmental Science & Technology*, 44(2), 668–674. <https://doi.org/10.1021/es902003f>
- Marques, M., Mari, M., Sierra, J., Nadal, M., & Domingo, J. L. (2017). Solar radiation as a swift pathway for PAH photodegradation: A field study. *Science of the Total Environment*, 581–582, 530–540. <https://doi.org/10.1016/j.scitotenv.2016.12.161>
- Marques, M., Cervello, D., Mari, M., Sierra, J., Schuhmacher, M., Domingo, J. L., & Nadal, M. (2020). The role of iron oxide on the photodegradation of polycyclic aromatic hydrocarbons: characterization and toxicity. *Polycyclic Aromatic Compounds*, 40(2), 524–534. <https://doi.org/10.1080/10406638.2018.1458743>
- Miller, J. S., & Olejnik, D. (2001). Photolysis of polycyclic aromatic hydrocarbons in water. *Water Research*, 35(1), 233–243. [https://doi.org/10.1016/S0043-1354\(00\)00230-X](https://doi.org/10.1016/S0043-1354(00)00230-X)
- Nogueira, F. G. E., Lopes, J. H., Silva, A. C., Lago, R. M., Fabris, J. D., & Oliveira, L. C. A. (2011). Catalysts based on clay and iron oxide for oxidation of toluene. *Applied Clay Science*, 51(3), 385–389. <https://doi.org/10.1016/j.clay.2010.12.007>
- Nguyen, V. H., Thi, L. A. P., Le, Q. V., Singh, P., Raizada, P., & Kajitvichyanukul, P. (2020). Tailored photocatalysts and revealed reaction pathways for photodegradation of polycyclic aromatic hydrocarbons (PAHs) in water, soil and other sources. *Chemosphere*, 260, 127529. <https://doi.org/10.1016/j.chemosphere.2020.127529>
- Ni, Z., Zhang, C., Wang, Z. Q., Zhao, S., Fan, X. Y., & Jia, H. Z. (2021). Performance and potential mechanism of transformation of polycyclic aromatic hydrocarbons (PAHs) on various iron oxides. *Journal of Hazardous Materials*, 403, 123993. <https://doi.org/10.1016/j.jhazmat.2020.123993>
- Premnath, N., Mohanrasu, K., Rao, R. G. R., Dinesh, G. H., Prakash, G. S., Ananthi, V., Ponnuchamy, K., Muthusamy, G., & Arun, A. (2021). A crucial review on polycyclic aromatic Hydrocarbons: Environmental occurrence and strategies for microbial degradation . *Chemosphere*, 280, 130608. <https://doi.org/10.1016/j.chemosphere.2021.130608>
- Qu, X. L., Liu, P., & Zhu, D. Q. (2008). Enhanced sorption of polycyclic aromatic hydrocarbons to tetra-alkyl ammonium modified smectites via cation-pi interactions . *Environmental Science & Technology*, 42(4), 1109–1116. <https://doi.org/10.1021/es071613f>
- Rani, M., & Rachna, S. U. (2020). Metal oxide-chitosan based nanocomposites for efficient degradation of carcinogenic PAHs. *Journal of Environmental Chemical Engineering*, 8, 103810. <https://doi.org/10.1016/j.jece.2020.103810>
- Rababah, A., & Matsuzawa, S. (2002). Treatment system for solid matrix contaminated with fluoranthene. II. Recirculating photodegradation technique. *Chemosphere*, 46(1), 49–57. [https://doi.org/10.1016/S0045-6535\(01\)00090-X](https://doi.org/10.1016/S0045-6535(01)00090-X)
- Ranc, B., Faure, P., Croze, V., & Simonnot, M. (2016). Selection of oxidant doses for in situ chemical oxidation of soils contaminated by polycyclic aromatic hydrocarbons (PAHs): A review. *Journal of Hazardous Materials*, 312, 280–297. <https://doi.org/10.1016/j.jhazmat.2016.03.068>
- Rivas, F. J. (2006). Polycyclic aromatic hydrocarbons sorbed on soils: a short review of chemical oxidation based treatments. *Journal of Hazardous Materials*, 138(2), 234–251. <https://doi.org/10.1016/j.jhazmat.2006.07.048>
- Rivas, F. J., Beltran, F. J., & Acedo, B. (2000). Chemical and photochemical degradation of acenaphthylene: Intermediate identification. *Journal of Hazardous Materials*, 75(1), 89–98. [https://doi.org/10.1016/S0304-3894\(00\)00196-5](https://doi.org/10.1016/S0304-3894(00)00196-5)
- Roncevic, S., Spasojevic, J., Maletic, S., Jazic, J. M., Isakovski, M. K., Agbaba, J., Grgic, M., & Dalmacija, B. (2016). Assessment of the bioavailability and phytotoxicity of sediment spiked with polycyclic aromatic hydrocarbons. *Environmental Science and Pollution Research International*, 23(4), 3239–3246. <https://doi.org/10.1007/s11356-015-5566-4>
- Rooney, J. J., & Pink, R. C. (1962). Formation and stability of hydrocarbon radical-ions on a silica-alumina surface. *Transactions of the Faraday Society*, 58, 1632–1641. <https://doi.org/10.1039/TF9625801632>
- Rupert, J. P. (1973). Electron spin resonance spectra of interlamellar copper(II)-arene complexes on montmorillonite. *The Journal of Physical Chemistry*, 77(6), 784–790. <https://doi.org/10.1021/j100625a011>
- Schaffer, A., Kastner, M., & Trapp, S. (2018). A unified approach for including non-extractable residues (NER) of chemicals and pesticides in the assessment of persistence. *Environmental Sciences Europe*, 30(1), 51.

- Soderstrom, G., Sellstrom, U., De Wit, C. A., & Tysklind, M. (2004). Photolytic debromination of decabromodiphenyl ether (BDE 209). *Environmental Science & Technology*, 38(1), 127–132. <https://doi.org/10.1021/es034682c>
- Sun, Y. Q., Xiong, X. N., He, M. J., Xu, Z. B., Hou, D. Y., Zhang, W. H., Ok, Y. S., Rinklebe, J., Wang, L. L., & Tsang, D. C. W. (2021). Roles of biochar-derived dissolved organic matter in soil amendment and environmental remediation: A critical review. *Chemical Engineering Journal*, 424, 130387. <https://doi.org/10.1016/j.cej.2021.130387>
- Sun, Z., Feng, L., Fang, G., Chu, L., Zhou, D., & Gao, J. (2021). Nano Fe<sub>2</sub>O<sub>3</sub> embedded in montmorillonite with citric acid enhanced photocatalytic activity of nanoparticles towards diethyl phthalate. *Journal of Environmental Sciences (China)*, 101, 248–259. <https://doi.org/10.1016/j.jes.2020.08.019>
- Sun, X. K., Bai, J., & Dong, D. B. (2021). Influence factors of enhanced photosensitized degradation of PAHs on soil surface using humic acid under UV irradiation. *Polycyclic Aromatic Compounds*, 41(8), 1739–1748. <https://doi.org/10.1080/10406638.2019.1695218>
- Shahsavari, E., Schwarz, A., Aiburto-Medina, A., & Ball, A. S. (2019). Biological degradation of polycyclic aromatic compounds (PAHs) in soil: A current perspective. *Current Pollution Reports*, 5(3), 84–92. <https://doi.org/10.1007/s40726-019-00113-8>
- Stangroom, S. J., Collins, C. D., & Lester, J. N. (2000). Abiotic Behaviour of organic micropollutants in soils and the aquatic environment. A review: II. Transformations. *Environmental Technology*, 21(8), 865–882. <https://doi.org/10.1080/09593332108618059>
- Samanta, S. K., Singh, O. V., & Jain, R. K. (2002). Polycyclic aromatic hydrocarbons: environmental pollution and bioremediation. *Trends in Biotechnology*, 20(6), 243–248. [https://doi.org/10.1016/S0167-7799\(02\)01943-1](https://doi.org/10.1016/S0167-7799(02)01943-1)
- Schaefer, C. E., Towne, R. M., Lippincott, D. R., Lazouskaya, V., Fischer, T. B., Bishop, M. E., & Dong, H. (2013). Coupled diffusion and abiotic reaction of trichlorethene in minimally disturbed rock matrices. *Environmental Science & Technology*, 47(9), 4291–4298. <https://doi.org/10.1021/es400457s>
- Schwarzenbach, R. P., Gschwend, P. M., & Imboden, D. M. (2003). Environmental organic chemistry, 2nd Edition. *Journal of Chemical Education*, 80, 1143.
- Si, Y. B., Wang, S. Q., Zhou, D. M., & Chen, H. M. (2004). Adsorption and photo-reactivity of bensulfuron-methyl on homoionite. *Clays and Clay Minerals*, 52(6), 742–748. <https://doi.org/10.1346/CCMN.2004.0520609>
- Si, Y. B., Zhou, J., Chen, H. M., Zhou, D. M., & Yue, Y. D. (2004). Effects of humic substances on photodegradation of bensulfuron-methyl on dry soil surfaces. *Chemosphere*, 56(10), 967–972. <https://doi.org/10.1016/j.chemosphere.2004.04.059>
- Solomon, D. H. (1968). Clay minerals as electron acceptors and/or electron donors in organic reactions. *Clays and Clay Minerals*, 16(1), 31–31. <https://doi.org/10.1346/CCMN.1968.0160105>
- Sun, X., Liu, H., Zhang, Y. B., Zhao, Y. Z., & Quan, X. (2011). Effects of Cu(II) and humic acid on atrazine photodegradation. *Journal of Environmental Sciences*, 23(5), 773–777. [https://doi.org/10.1016/S1001-0742\(10\)60476-7](https://doi.org/10.1016/S1001-0742(10)60476-7)
- Szaciłowski, K., Macyk, W., Drzewiecka-Matuszek, A., Brindell, M., & Stochel, G. (2005). Bioinorganic photochemistry: frontiers and mechanisms. *Chemical Reviews*, 105(6), 2647–2694. <https://doi.org/10.1021/cr030707e>
- Tamamura, S., Sato, T., Ota, Y., Tang, N., & Hayakawa, K. (2010). Decomposition of polycyclic aromatic hydrocarbon (PAHs) on mineral surface under controlled relative humidity. *Acta Geologica Sinica - English Edition*, 80(2), 185–191. <https://doi.org/10.1111/j.1755-6724.2006.tb00229.x>
- Trombetta, M., Busca, G., Lenarda, M., Storaro, L., Ganzerla, R., Piovesan, L., Jimenez Lopez, A., Alcantara-Rodriguez, M., & Rodríguez-Castellón, E. (2000). Solid acid catalysts from clays: Evaluation of surface acidity of mono- and bi-pillared smectites by FTIR spectroscopy measurements, NH<sub>3</sub>-TPD and catalytic tests. *Applied Catalysis A: General*, 193(1-2), 55–69. [https://doi.org/10.1016/S0926-860X\(99\)00413-5](https://doi.org/10.1016/S0926-860X(99)00413-5)
- U.S., E.P.A. (2009). Office of Underground Storage Tanks. Use of Monitored Natural Attenuation at Superfund, RCRA Corrective Action, and Underground Storage Tank Sites; OSWER Directive 9200.4-17.
- Vidal, C. B., dos Santos, A. B., do Nascimento, R. F., & Bandosz, T. J. (2015). Reactive adsorption of pharmaceuticals on tin oxide pillared montmorillonite: Effect of visible light exposure. *Chemical Engineering Journal*, 259, 865–875. <https://doi.org/10.1016/j.cej.2014.07.079>
- Wincent, E., Jönsson, M. E., Bottai, M., Lundstedt, S., & Dreij, K. (2015). Aryl Hydrocarbon Receptor Activation and Developmental Toxicity in Zebrafish in Response to Soil Extracts Containing Unsubstituted and Oxygenated PAHs. *Environmental Science & Technology*, 49(6), 3869–3877. <https://doi.org/10.1021/es505588s>
- Wang, C., Li, Y. Z., Tan, H., Zhang, A. K., Xie, Y. L., Wu, B., & Xu, H. (2019). A novel microbe consortium, nano-visible light photocatalyst and microcapsule system to degrade PAHs. *Chemical Engineering Journal*, 359, 1065–1074. <https://doi.org/10.1016/j.cej.2018.11.077>
- Wang, C., Yu, D., Shi, W., Jiao, K., Wu, B., & Xu, H. (2016). Application of spent mushroom (*Lentinula edodes*) substrate and acclimated sewage sludge on the bioremediation of polycyclic aromatic hydrocarbon polluted soil. *RSC Advances*, 6(43), 37274–37285. <https://doi.org/10.1039/C6RA05457A>
- Wang, M. C., & Huang, P. M. (1989). Pyrogallol transformations as catalyzed by nontronite, bentonite, and kaolinite. *Clays and Clay Minerals*, 37(6), 525–531. <https://doi.org/10.1346/CCMN.1989.0370604>

- Wang, Y., Liu, C. S., Li, F. B., Liu, C. P., & Liang, J. B. (2009). Photodegradation of polycyclic aromatic hydrocarbon pyrene by iron oxide in solid phase. *Journal of Hazardous Materials*, 162(2-3), 716–723. <https://doi.org/10.1016/j.jhazmat.2008.05.086>
- Wang, Z., Jia, H. Z., Zheng, T., Dai, Y. C., Zhang, C., Guo, X. T., Wang, T. C., & Zhu, L. Y. (2020). Promoted catalytic transformation of polycyclic aromatic hydrocarbons by MnO<sub>2</sub> polymorphs: Synergistic effects of Mn<sup>3+</sup> and oxygen vacancies. *Applied Catalysis B: Environmental*, 272, 119030–119038. <https://doi.org/10.1016/j.apcatb.2020.119030>
- Weigand, H., Totsche, K. U., Kögel-Knabner, I., Annweiler, E., Richnow, H. H., & Michaelis, W. (2002). Fate of anthracene in contaminated soil: transport and biochemical transformation under unsaturated flow conditions. *European Journal of Soil Science*, 53(1), 71–81. <https://doi.org/10.1046/j.1365-2389.2002.00427.x>
- Wenk, J., & Canonica, S. (2012). Phenolic antioxidants inhibit the triplet-induced transformation of anilines and sulfonamide antibiotics in aqueous solution. *Environmental Science & Technology*, 46(10), 5455–5462. <https://doi.org/10.1021/es300485u>
- Wild, S. R., & Jones, K. C. (1995). Polynuclear aromatic hydrocarbons in the United Kingdom environment: A preliminary source inventory and budget. *Environmental Pollution (Barking, Essex: 1987)*, 88(1), 91–108. [https://doi.org/10.1016/0269-7491\(95\)91052-M](https://doi.org/10.1016/0269-7491(95)91052-M)
- Wu, F., Li, J., Peng, Z. E., & Deng, N. S. (2008). Photochemical formation of hydroxyl radicals catalyzed by montmorillonite. *Chemosphere*, 72(3), 407–413. <https://doi.org/10.1016/j.chemosphere.2008.02.034>
- Qin, C., Troya, D., Shang, C., Hildreth, S., Helm, R., & Xia, K. (2015). Surface catalyzed oxidative oligomerization of 17β-estradiol by Fe(3+)-saturated montmorillonite. *Environmental Science & Technology*, 49(2), 956–964. <https://doi.org/10.1021/es504815t>
- Xiao, L., Qu, X. L., & Zhu, D. Q. (2007). Biosorption of nonpolar hydrophobic organic compounds to escherichia coli facilitated by metal and proton surface binding. *Environmental Science & Technology*, 41(8), 2750–2755. <https://doi.org/10.1021/es062343o>
- Xu, X., Xiao, R. Y., Dionysiou, D. D., Spinney, R., Fu, T., Li, Q., Wang, Z. J., Wang, D. H., & Wei, Z. S. (2018). Kinetics and mechanisms of the formation of chlorinated and oxygenated polycyclic aromatic hydrocarbons during chlorination. *Chemical Engineering Journal*, 351, 248–257. <https://doi.org/10.1016/j.ccej.2018.06.075>
- Yao, X. L., Wang, K., Wang, W., Zhang, T. T., Wang, W., Yang, X. Y., Qian, F., & Li, H. L. (2020). Reduction of polycyclic aromatic hydrocarbons (PAHs) emission from household coal combustion using ferrous oxide as a coal burning additive. *Chemosphere*, 252, 126489. <https://doi.org/10.1016/j.chemosphere.2020.126489>
- Yuan, S. H., Liu, X. X., Liao, W. J., Zhang, P., Wang, X. M., & Tong, M. (2018). Mechanisms of electron transfer from structural Fe(II) in reduced nontronite to oxygen for production of hydroxyl radicals. *Geochimica et Cosmochimica Acta*, 223, 422–436. <https://doi.org/10.1016/j.gca.2017.12.025>
- Yang, Y., Zhang, N., Xu, e M., & Tao, S. (2010). Impact of soil organic matter on the distribution of polycyclic aromatic hydrocarbons (PAHs) in soils. *Environmental Pollution (Barking, Essex: 1987)*, 158(6), 2170–2174. <https://doi.org/10.1016/j.envpol.2010.02.019>
- Yap, C. L., Gan, S., & Ng, H. K. (2011). Fenton based remediation of polycyclic aromatic hydrocarbons-contaminated soils. *Chemosphere*, 83(11), 1414–1430. <https://doi.org/10.1016/j.chemosphere.2011.01.026>
- Yi, H., & Crowley, D. E. (2007). Biostimulation of PAH degradation with plants containing high concentrations of linoleic acid. *Environmental Science & Technology*, 41(12), 4382–4388. <https://doi.org/10.1021/es062397y>
- Zhang, C. F., & Katayama, A. (2012). Humic as an electron mediator for microbial reductive dehalogenation. *Environmental Science & Technology*, 46(12), 6575–6583. <https://doi.org/10.1021/es3002025>
- Zhang, L. H., Li, P. J., Gong, Z. Q., & Li, X. M. (2008). Photocatalytic degradation of polycyclic aromatic hydrocarbons on soil surfaces using TiO<sub>2</sub> under UV light. *Journal of Hazardous Materials*, 158(2-3), 478–484. <https://doi.org/10.1016/j.jhazmat.2008.01.119>
- Zhang, L. H., Li, P. J., Gong, Z. Q., & Oni, A. A. (2006). Photochemical behavior of benzo[a]pyrene on soil surfaces under UV light irradiation. *Journal of Environmental Sciences*, 18(6), 1226–1232. [https://doi.org/10.1016/S1001-0742\(06\)60067-3](https://doi.org/10.1016/S1001-0742(06)60067-3)
- Zhang, L. H., Xu, C. B., Chen, Z. L., Li, X. M., & Li, P. J. (2010). Photodegradation of pyrene on soil surfaces under UV light irradiation. *Journal of Hazardous Materials*, 173(1-3), 168–172. <https://doi.org/10.1016/j.jhazmat.2009.08.059>
- Zhang, W. H., Zhuang, L. W., Yuan, Y., Tong, L. Z., & Tsang, D. C. W. (2011). Enhancement of phenanthrene adsorption on a clayey soil and clay minerals by coexisting lead or cadmium. *Chemosphere*, 83(3), 302–310. <https://doi.org/10.1016/j.chemosphere.2010.12.056>
- Zhang, X., Wu, F., Deng, N. S., Pozdnyakov, I. P., Glebov, E. M., Grivin, V. P., Plyusnin, V. F., & Bazhin, N. N. (2008). Evidence of the hydroxyl radical formation upon the photolysis of an iron-rich clay in aqueous solutions. *Reaction Kinetics and Catalysis Letters*, 94(2), 207–218. <https://doi.org/10.1007/s11144-008-5342-2>
- Zhang, Z. G., Kyotani, T., & Tomita, A. (1989). Dynamic behavior of surface oxygen complexes during oxygen-chemisorption and subsequent temperature-programmed desorption of calcium-loaded coal chars. *Energy & Fuels*, 3(5), 566–571. <https://doi.org/10.1021/ef00017a006>



- Zhang, P., Yuan, S. H., & Liao, P. (2016). Mechanisms of hydroxyl radical production from abiotic oxidation of pyrite under acidic conditions. *Geochimica et Cosmochimica Acta*, 172, 444–457. <https://doi.org/10.1016/j.gca.2015.10.015>
- Zhao, S., Jia, H. Z., Nulaji, G., Gao, H. W., Wang, F., & Wang, C. Y. (2017). Photolysis of polycyclic aromatic hydrocarbons (PAHs) on Fe<sup>3+</sup>-montmorillonite surface under visible light: Degradation kinetics, mechanism, and toxicity assessments. *Chemosphere*, 184, 1346–1354. <https://doi.org/10.1016/j.chemosphere.2017.06.106>
- Zhao, S., Miao, D., Zhu, K. C., Tao, K. L., Wang, C. Y., Sharma, V. K., & Jia, H. Z. (2019). Interaction of benzo[a]pyrene with Cu(II)-montmorillonite: Generation and toxicity of environmentally persistent free radicals and reactive oxygen species. *Environment International*, 129, 154–163. <https://doi.org/10.1016/j.envint.2019.05.037>
- Zhu, D. Q., Herbert, B. E., Schlautman, M. A., Carraway, E. R., & Jin, H. (2004). Cation-pi bonding: A new perspective on the sorption of polycyclic aromatic hydrocarbons to mineral surfaces. *Journal of Environmental Quality*, 33(4), 1322–1330. <https://doi.org/10.2134/jeq2004.1322>

## Abiotic transformation of polycyclic aromatic hydrocarbons via interaction with soil components: A systematic review

Jinbo Liu<sup>a</sup>, Chi Zhang<sup>a</sup>, Hanzhong Jia<sup>a\*</sup>, Eric Lichtfouse<sup>b</sup>, Virender K. Sharma<sup>c</sup>

<sup>a</sup> Key Laboratory of Plant Nutrition and the Agri-environment in Northwest China, Ministry of Agriculture, College of Natural Resources and Environment, Northwest A & F University, Yangling 712100, China

<sup>b</sup> Aix-Marseille Univ, CNRS, IRD, INRA, CEREGE, Aix-en-Provence 13100, France

<sup>c</sup> Program for the Environment and Sustainability, Department of Occupational and Environmental Health, School of Public Health, Texas A&M University, College Station, TX 77843, USA

\* Corresponding author E-mails: [jiahz@nwafu.edu.cn](mailto:jiahz@nwafu.edu.cn)

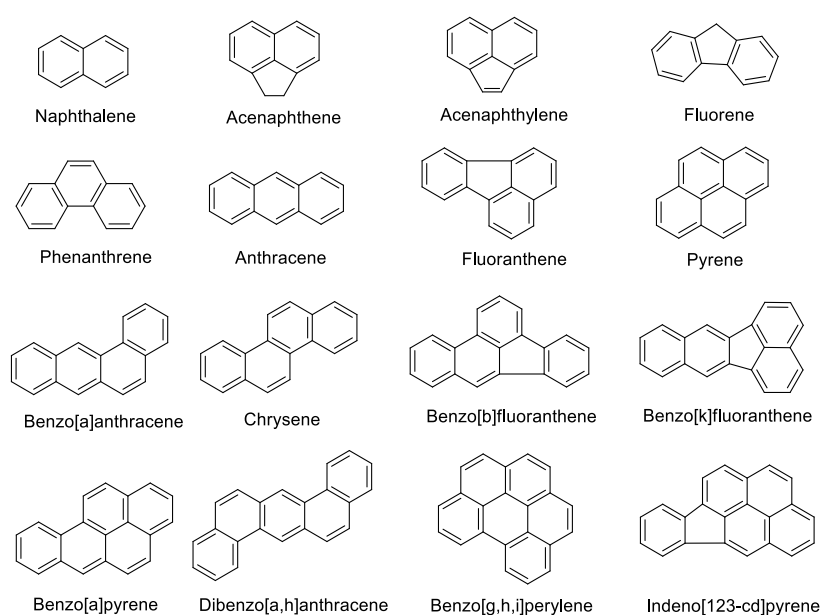


**Figure S1.** Chemical structures of 16 polycyclic aromatic hydrocarbons (PAHs) considered as priority pollutants by the US Environmental Protection Agency (EPA).

**Table S1.** Comparison of photodegradation of polycyclic aromatic hydrocarbons (PAHs) in soils

PAHs	Soil moieties	Kinetics ( $k_{obs}$ , $d^{-1}$ or $h^{-1}$ ) or Transformation rate	Products	Ref.
Anthracene	Fe <sup>3+</sup> , Al <sup>3+</sup> , Cu <sup>2+</sup> , Ca <sup>2+</sup> , K <sup>+</sup> and Na <sup>+</sup> modified smectite clays	k: 0.154 h <sup>-1</sup> for Na <sup>+</sup> -smectite, 0.168 h <sup>-1</sup> for K <sup>+</sup> -smectite, 0.181 h <sup>-1</sup> for Ca <sup>2+</sup> -smectite, 0.255 h <sup>-1</sup> for Cu <sup>2+</sup> -smectite, 0.339 h <sup>-1</sup> for Al <sup>3+</sup> -smectite, 0.405 h <sup>-1</sup> for Fe <sup>3+</sup> -smectite, k: 5.3*10 <sup>-3</sup> h <sup>-1</sup> for 0.5 wt.% TiO <sub>2</sub> , 5.4*10 <sup>-3</sup> h <sup>-1</sup> for 1 wt.% TiO <sub>2</sub> ,	Not shown	Jia et al., 2015
Phenanthrene	Soil and 0.5-3 wt.% TiO <sub>2</sub>	6.0*10 <sup>-3</sup> h <sup>-1</sup> for 2 wt.% TiO <sub>2</sub> , 5.1*10 <sup>-3</sup> h <sup>-1</sup> for 3 wt.% TiO <sub>2</sub> , 1.3*10 <sup>-3</sup> h <sup>-1</sup> for control k: 3.6*10 <sup>-3</sup> h <sup>-1</sup> for 0.5 wt.% TiO <sub>2</sub> , 3.7*10 <sup>-3</sup> h <sup>-1</sup> for 1 wt.% TiO <sub>2</sub> ,	Not shown	Zhang et al., 2008a
Pyrene	Soil and 0.5-3 wt.% TiO <sub>2</sub>	3.7*10 <sup>-3</sup> h <sup>-1</sup> for 2 wt.% TiO <sub>2</sub> , 3.6*10 <sup>-3</sup> h <sup>-1</sup> for 3 wt.%TiO <sub>2</sub> , 1.1*10 <sup>-3</sup> h <sup>-1</sup> for control k: 6.7*10 <sup>-3</sup> h <sup>-1</sup> for 0.5 wt.% TiO <sub>2</sub> ,	Not shown	Zhang et al., 2008a
Benzo[a]pyrene	Soil and 0.5-3 wt.% TiO <sub>2</sub>	7.2*10 <sup>-3</sup> h <sup>-1</sup> for 1 wt.% TiO <sub>2</sub> , 7.8*10 <sup>-3</sup> h <sup>-1</sup> for 2 wt.% TiO <sub>2</sub> , 7.3*10 <sup>-3</sup> h <sup>-1</sup> for 3 wt.% TiO <sub>2</sub> , 1.9*10 <sup>-3</sup> h <sup>-1</sup> for control k: 0.0113 h <sup>-1</sup> for 5 mg kg <sup>-1</sup> , 0.0102 h <sup>-1</sup> for 10 mg kg <sup>-1</sup> , 0.0088 h <sup>-1</sup> for 20 mg kg <sup>-1</sup> , 0.0071 h <sup>-1</sup> for 40 mg kg <sup>-1</sup> , 0.0060 for control	Not shown	Zhang et al., 2008a
Phenanthrene	Soil and 5-40 mg kg <sup>-1</sup> humic acids	k: 0.0179 h <sup>-1</sup> for 5 mg kg <sup>-1</sup> , 0.0151 h <sup>-1</sup> for 10 mg kg <sup>-1</sup> , 0.0132 h <sup>-1</sup> for 20 mg kg <sup>-1</sup> , 0.0119 h <sup>-1</sup> for 40 mg kg <sup>-1</sup> , 0.0037 for control	Not shown	Zhang et al., 2008a
Pyrene	Soil and 5-40 mg kg <sup>-1</sup> humic acids	k: 0.0236 h <sup>-1</sup> for 5 mg kg <sup>-1</sup> , 0.0212 h <sup>-1</sup> for 10 mg kg <sup>-1</sup> , 0.0194 h <sup>-1</sup> for 20 mg kg <sup>-1</sup> , 0.0180 h <sup>-1</sup> for 40 mg kg <sup>-1</sup> , 0.0078 for control	Not shown	Zhang et al., 2008a
Benzo[a]pyrene	Soil and 5-40 mg kg <sup>-1</sup> humic acids	0.0180 h <sup>-1</sup> for 40 mg kg <sup>-1</sup> , 0.0078 for control	Not shown	Zhang et al., 2008a
Anthracene	Red earth, latosol,	k: 0.758 d <sup>-1</sup> for calcic brown	Anthraquinone	Jia et al.,

	fluvo-aquic soil, yellow earth, chernozem, brown soil, calcic brown soil	soil, 3.161 d <sup>-1</sup> for brown soil, 3.322 d <sup>-1</sup> for chernozem, 3.861 d <sup>-1</sup> for fluvo-aquic soil, 5.977 d <sup>-1</sup> for yellow earth, 6.082 d <sup>-1</sup> for latosol, 7.364 d <sup>-1</sup> for red earth. Photodegradation rate follows the order of Fe <sup>3+</sup> -smectite > Cu <sup>2+</sup> -smectite >> Ca <sup>2+</sup> - smectite > K <sup>+</sup> -smectite > Na <sup>+</sup> - smectite.		2018a
Phenanthrene	Fe <sup>3+</sup> , Cu <sup>2+</sup> , Ca <sup>2+</sup> , K <sup>+</sup> and Na <sup>+</sup> modified smectite clays	k: 0.2338 h <sup>-1</sup> for Fe(III)- Kaolinite, 0.3527 h <sup>-1</sup> for Fe(III)- Vermiculite, 0.4094 h <sup>-1</sup> for Fe(III)-Semctite	Not shown	Jia et al., 2012
Phenanthrene	Fe(III)-Smectite Fe(III)-Vermiculite Fe(III)-Kaolinite	k: 1.37*10 <sup>-2</sup> h <sup>-1</sup> for 1 wt.% TiO <sub>2</sub> , 1.47*10 <sup>-2</sup> h <sup>-1</sup> for 2 wt.% TiO <sub>2</sub> , 1.42*10 <sup>-2</sup> h <sup>-1</sup> for 3 wt.% TiO <sub>2</sub> , 1.39*10 <sup>-2</sup> h <sup>-1</sup> for 4 wt.% TiO <sub>2</sub> , 1.31*10 <sup>-2</sup> h <sup>-1</sup> for control	9,10- Phenanthrenequinone, phthalates,	Jia et al., 2012
Phenanthrene	Soil and 1-4 wt.% TiO <sub>2</sub>	k: 1.62*10 <sup>-2</sup> h <sup>-1</sup> for 1 wt.% TiO <sub>2</sub> , 1.75*10 <sup>-2</sup> h <sup>-1</sup> for 2 wt.% TiO <sub>2</sub> , 1.70*10 <sup>-2</sup> h <sup>-1</sup> for 3 wt.% TiO <sub>2</sub> , 1.63*10 <sup>-2</sup> h <sup>-1</sup> for 4 wt.% TiO <sub>2</sub> , 1.51*10 <sup>-2</sup> h <sup>-1</sup> for control	Not shown	Dong et al., 2010
Pyrene	Soil and 1-4 wt.% TiO <sub>2</sub>	k: 1.54*10 <sup>-2</sup> h <sup>-1</sup> for 10 mg kg <sup>-1</sup> humic acids, 1.65*10 <sup>-2</sup> h <sup>-1</sup> for 20 mg kg <sup>-1</sup> humic acids, 1.70*10 <sup>-2</sup> h <sup>-1</sup> for 30 mg kg <sup>-1</sup> humic acids, 1.73*10 <sup>-2</sup> h <sup>-1</sup> for 40 mg kg <sup>-1</sup> humic acids, 1.47*10 <sup>-2</sup> h <sup>-1</sup> for control.	Not shown	Dong et al., 2010
Phenanthrene	Soil and 10-40 mg kg <sup>-1</sup> humic acids	k: 1.86*10 <sup>-2</sup> h <sup>-1</sup> for 10 mg kg <sup>-1</sup> humic acids, 1.90*10 <sup>-2</sup> h <sup>-1</sup> for 20 mg kg <sup>-1</sup> humic acids, 1.92*10 <sup>-2</sup> h <sup>-1</sup> for 30 mg kg <sup>-1</sup> humic acids, 1.95*10 <sup>-2</sup> h <sup>-1</sup> for 40 mg kg <sup>-1</sup> humic acids, 1.75*10 <sup>-2</sup> h <sup>-1</sup> for control.	Not shown	Dong et al., 2010
Pyrene	Soil and 10-40 mg kg <sup>-1</sup> humic acids	k: 1.06*10 <sup>-2</sup> h <sup>-1</sup> for 119μW/cm <sup>2</sup> , 1.47*10 <sup>-2</sup> h <sup>-1</sup> for 238μW/cm <sup>2</sup> , 1.77*10 <sup>-2</sup> h <sup>-1</sup> for 357μW/cm <sup>2</sup>	Not shown	Dong et al., 2010
Phenanthrene	Soil and 119–357 μW/cm <sup>2</sup> UV light intensity	k: 1.26*10 <sup>-2</sup> h <sup>-1</sup> for 119μW/cm <sup>2</sup> , 1.75*10 <sup>-2</sup> h <sup>-1</sup> for 238μW/cm <sup>2</sup> ,	Not shown	Dong et al., 2010
Pyrene	Soil and 119–357 μW/cm <sup>2</sup>			

	UV light intensity	1.92*10 <sup>-2</sup> h <sup>-1</sup> for 357μW/cm <sup>2</sup> k: 0.0391 d <sup>-1</sup> for 4.0 mm soil depth, 0.0438 d <sup>-1</sup> for 2.4 mm soil depth, 0.0458 d <sup>-1</sup> for 2.0 mm soil depth, 0.0465 d <sup>-1</sup> for 1.6 mm soil depth, 0.0524 d <sup>-1</sup> for 1.0 mm soil depth,			
Benzo[a]pyrene	1-4 mm soil depth		Not shown	Zhang et al., 2006	
Benzo[a]pyrene	Soil and 0.5-3 wt.% TiO <sub>2</sub>	k: 6.713*10 <sup>-3</sup> h <sup>-1</sup> for 0.5 wt.% TiO <sub>2</sub> , 7.225*10 <sup>-3</sup> h <sup>-1</sup> for 1.0 wt.% TiO <sub>2</sub> , 7.758*10 <sup>-3</sup> h <sup>-1</sup> for 2.0 wt.% TiO <sub>2</sub> , 7.300*10 <sup>-3</sup> h <sup>-1</sup> for 3 wt.% TiO <sub>2</sub> , 1.908*10 <sup>-3</sup> h <sup>-1</sup> for control k: 6.246*10 <sup>-3</sup> h <sup>-1</sup> for 2 wt.% Fe <sub>2</sub> O <sub>3</sub> , 6.771*10 <sup>-3</sup> h <sup>-1</sup> for 5 wt.%	Not shown	Zhang et al., 2006	
Benzo[a]pyrene	Soil and 2-10 wt.% Fe <sub>2</sub> O <sub>3</sub>	Fe <sub>2</sub> O <sub>3</sub> , 6.942*10 <sup>-3</sup> h <sup>-1</sup> for 7 wt.% Fe <sub>2</sub> O <sub>3</sub> , 6.675*10 <sup>-3</sup> h <sup>-1</sup> for 10 wt.% Fe <sub>2</sub> O <sub>3</sub> , 1.908*10 <sup>-3</sup> h <sup>-1</sup> for control	Not shown	Zhang et al., 2006	
Pyrene	0-1 mm soil particle sizes	The rates of pyrene photodegradation at different soil particle size followed the order: less than 1 mm > less than 0.45 mm > less than 0.25 mm. k: 0.035 d <sup>-1</sup> for 1.0 mm soil depth, 0.0301 d <sup>-1</sup> for 1.6 mm soil depth, 0.0252 d <sup>-1</sup> for 2.0 mm soil depth, 0.0215 d <sup>-1</sup> for 2.4 mm soil depth, 0.0185 d <sup>-1</sup> for 4.0 mm soil depth.	Not shown	Zhang et al., 2010	
Pyrene	1-4 mm soil depth		Not shown	Zhang et al., 2010	
Pyrene	Soil and 5-40 mg kg <sup>-1</sup> humic acids	k: 0.0062 h <sup>-1</sup> for 5 mg kg <sup>-1</sup> humic acids, 0.0054 h <sup>-1</sup> for 10 mg kg <sup>-1</sup> humic acids, 0.0049 h <sup>-1</sup> for 20 mg kg <sup>-1</sup> humic acids, 0.0041 h <sup>-1</sup> for 40 mg kg <sup>-1</sup> humic acids, 0.0011 h <sup>-1</sup> for control.	Not shown	Zhang et al., 2010	
Pyrene	α-FeOOH	k: 0.1829 h <sup>-1</sup> for γ-Fe <sub>2</sub> O <sub>3</sub> ,	Pyreno	Wang et al.,	

	$\alpha$ -Fe <sub>2</sub> O <sub>3</sub>	0.1864 for $\gamma$ -FeOOH,		2009
	$\gamma$ -Fe <sub>2</sub> O <sub>3</sub>	0.2084 for $\alpha$ -Fe <sub>2</sub> O <sub>3</sub> ,		
	$\gamma$ -FeOOH	0.2301 for $\alpha$ -FeOOH		
		k: 0.2571 h <sup>-1</sup> for 5 g/m <sup>2</sup> $\alpha$ -FeOOH,		
		0.2369 h <sup>-1</sup> for 10 g/m <sup>2</sup> $\alpha$ -FeOOH,		
Pyrene	Soil and 5-50 g/m <sup>2</sup> $\alpha$ -FeOOH	0.2301 h <sup>-1</sup> for 20 g/m <sup>2</sup> $\alpha$ -FeOOH,	Pyrene	Wang et al., 2009
		0.1694 h <sup>-1</sup> for 50 g/m <sup>2</sup> $\alpha$ -FeOOH,		
Pyrene	Soil and 480–4800 $\mu$ W/cm <sup>2</sup> UV light intensity	k: 0.2301 h <sup>-1</sup> for 119 $\mu$ W/cm <sup>2</sup> , 0.2390 h <sup>-1</sup> for 238 $\mu$ W/cm <sup>2</sup> , 0.2695 h <sup>-1</sup> for 357 $\mu$ W/cm <sup>2</sup>	Pyrene	Wang et al., 2009
		The photodegradation percentages of pyrene are 94.8, 97.7, and 100% for alluvial soil, red soil, and quartz sand, respectively.		
Pyrene	Quartz sand and alluvial and red soils with 5% (w/w) $\delta$ -MnO <sub>2</sub>		Not shown	Chien et al., 2011
Chrysene	Laponite	k: 4.35*10 <sup>-2</sup> min <sup>-1</sup>	Phthalic acid, 1,4-chrysenequinone, 1,4-chrysenediol, 2-formylbenzoic acid	Kong and Ferry 2003

**Note:** Kinetics ( $k_{obs}$ ) represents the photolysis rate of PAHs.

**Table S2.** Comparison of chemical oxidation of PAHs in soils

PAHs	Soil moieties	Kinetics ( $k_{obs}$ , $d^{-1}$ or $h^{-1}$ ) or Transformation rate	Products	Ref.
Fluoranthene	Clay	Transformation rate: 71.4% of the initial carbon was transformed.	High molecular weight compounds and carbonaceous residue	Ghislain et al., 2010
Fluoranthene	Limestone	Transformation rate: 17.1% of the initial carbon was transformed	High molecular weight compounds	Ghislain et al., 2010
Anthracene	Fe(III)-smectite, Fe(III)-illite, Fe(III)-pyrophyllite, Fe(III)-kaolinite	0.4424 $d^{-1}$ for Fe(III)-smectite, 0.0122 $d^{-1}$ for Fe(III)-illite, 0.0068 $d^{-1}$ for Fe(III)-pyrophyllite, 0.0002 $d^{-1}$ for Fe(III)-kaolinite	9,10-anthraquinone	Li et al., 2014
Pyrene	Alluvial and red soil with 5% (w/w) $\delta$ -MnO <sub>2</sub>	Transformation rate: 41.8% for alluvial soil, 35.8% for red soil.	Not shown	Chien et al., 2011
Anthracene	Ellerslie, Shale and Malmo soil and montmorillonite	Transformation rate: montmorillonite > Ellerslie > shale > Malmo	Bianthracene	Karimilofab ad et al., 1996
Anthracene	$\alpha$ -MnO <sub>2</sub> , $\beta$ -MnO <sub>2</sub> , $\gamma$ -MnO <sub>2</sub> , $\delta$ -MnO <sub>2</sub> , Amorphous MnO <sub>2</sub>	k: 0.180 $d^{-1}$ for Amorphous MnO <sub>2</sub> , 0.057 $d^{-1}$ for $\gamma$ -MnO <sub>2</sub> , 0.017 $d^{-1}$ for $\alpha$ -MnO <sub>2</sub> , 0.011 $d^{-1}$ for $\delta$ -MnO <sub>2</sub> , 0.002 $d^{-1}$ for $\beta$ -MnO <sub>2</sub>	Anthraquinone	Wang et al., 2020
Naphthalene	Amorphous MnO <sub>2</sub>	Transformation rate: Anthracene > Phenanthrene > Naphthalene	Not shown	Wang et al., 2020
Anthracene	Fe(III)-montmorillonite	Transformation rate: 30 %	9-anthranone, anthraquinone	Jia et al., 2014
Naphthalene	Fe(III)-montmorillonite	Transformation rate: insignificant changes	Not shown	Jia et al., 2014
Phenanthrene	Fe(III)-montmorillonite	Transformation rate: insignificant changes	Not shown	Jia et al., 2014
Chrysene	Fe(III)-montmorillonite	Transformation rate: insignificant changes	Not shown	Jia et al., 2014
Pyrene	Fe(III)-montmorillonite	Transformation rate: 50 %	Hydroxypyrene	Jia et al., 2014
Benzo[a]pyrene	Fe(III)-montmorillonite	Transformation rate: 70 %	Benzo[a]pyrene-12-one, Benzo[a]pyrene-6-one, Benzo[a]pyrene-6,12-quinone	Jia et al., 2014
Anthracene	Hectorite (SHCa-1), MMT (Swy-1), MMT (SAz-1), Saponite (SapCa-2)	k: 0.3410 $d^{-1}$ for SHCa-1, 0.2894 $d^{-1}$ for Swy-1, 0.2507 $d^{-1}$ for SAz-1, 0.2424 $d^{-1}$ , for SapCa-2,	9-anthranone, anthraquinone	Jia et al., 2014

	Illite	0.0122 d <sup>-1</sup> for Illite,		
	Pyrophyllite	0.0068 d <sup>-1</sup> for Pyrophyllite,		
	Kaolinite	0.0020 d <sup>-1</sup> for Kaolinite		
Anthracene	Fe(III)- montmorillonite	Transformation rate: 65 %	9-anthranone, anthraquinone	Jia et al., 2016
Phenanthrene	Fe(III)- montmorillonite	Transformation rate: insignificant changes	Not shown	Jia et al., 2016
Pyrene	Fe(III)- montmorillonite	Transformation rate: 90 %	Not shown	Jia et al., 2016
Benzo[a]pyrene	Fe(III)- montmorillonite	Transformation rate: 100 %	Not shown	Jia et al., 2016
Anthracene	0.02-0.10 M Vitamin C (VC)- reduced Humin (HM)	k: 0.0732 d <sup>-1</sup> for 0.02 M VC-HM, 0.1137 d <sup>-1</sup> for 0.04 M VC-HM, 0.1748 d <sup>-1</sup> for 0.08 M VC-HM, 0.1749 d <sup>-1</sup> for 0.10 M VC-HM, 0.0097 d <sup>-1</sup> for control	Not shown	Jia et al., 2020
Anthracene	0.02-0.10 M H <sub>2</sub> O <sub>2</sub> - HM	k: 0.0616 d <sup>-1</sup> for 0.02 M VC-HM, 0.0774 d <sup>-1</sup> for 0.04 M VC-HM, 0.1023 d <sup>-1</sup> for 0.08 M VC-HM, 0.1056 d <sup>-1</sup> for 0.10 M VC-HM 0.0097 d <sup>-1</sup> for control	Not shown	Jia et al., 2020
Naphthalene Phenanthrene Anthracene Benzo[a]pyrene	0.01 M VC-HM	k: 0.0253 d <sup>-1</sup> for naphthalene, 0.0299 d <sup>-1</sup> for phenanthrene, 0.0323 d <sup>-1</sup> for anthracene, 0.0373 d <sup>-1</sup> for benzo[a]pyrene	Not shown	(Jia et al., 2020)

**Note:** Kinetics ( $k_{obs}$ ) represents the oxidate transformation rate of PAHs, MMT means montmorillonite.